Characterising and detecting genuinely high-dimensional genuine multipartite entanglement

Gabriele Cobucci1 and Armin Tavakoli1

¹Physics Department and NanoLund, Lund University, Box 118, 22100 Lund, Sweden. (Dated: April 16, 2024)

Entangled states with both multiple local levels and multiple subsystems is increasingly entering state-of-the-art quantum technology. We investigate whether such high-dimensional multipartite entangled states can be simulated using only low-dimensional entanglement. To this end, we propose to benchmark the multipartite entanglement dimensionality via the worst-case bipartite entanglement dimension needed to generate the state as a mixture over the different bisections of the system. In order to detect this genuinely high-dimensional and genuinely multipartite entanglement, we develop several classes of general criteria. They are respectively based on fidelity measurements, efficient fidelity estimation using only a minimal number of measurements and convex programming methods. Our approach is a step towards understanding the role of entanglement dimensionality beyond the well-studied bipartite systems and our methods readily lend themselves to high-dimensional multipartite entanglement experiments.

I. INTRODUCTION

Detecting, quantifying and characterising relevant forms of entanglement is of central interest in quantum information science [1]. Many times, the most appropriate form of entanglement goes beyond simply defying separability. An important example is in systems of many qubits, where detecting entanglement does not reveal whether it is a feature of all the n qubits or confined to just a subset of them [2]. To ensure that the entanglement is truly n-partite, it is standard to instead consider the stronger notion of genuine multipartite entanglement (GME), which ensures that the state cannot be generated by entangling only some of the qubits. Naturally, much theoretical research has been invested in developing criteria for GME, see e.g. the review [3], and satisfying such criteria is a typical aim for multi-qubit entanglement experiments, see e.g. [4–11].

In recent years, high-dimensional systems have emerged as a major frontier for entanglement. In bipartite systems, entanglement has been detected far beyond qubit dimensions [12, 13]. The genuine dimensionality of entanglement present in a bipartite high-dimensional system is captured by its so-called Schmidt number [14]; it is the smallest dimension of entanglement required to simulate the state with free classical randomness. Naturally, many criteria have been developed to witness the Schmidt number (see e.g. [14–21]) and many experiments have used it as a benchmark for certifying genuinely high-dimensional bipartite entanglement [22–27].

However, the combination of high-dimensional and multipartite systems is more challenging, both from a theoretical and experimental point of view. Only recently have experiments reported on successful implementations of high-dimensional multipartite states on various platforms. Particular focus has been on the high-dimensional versions of the seminal Greenberger-Horne-Zeilinger (GHZ) states and cluster states [28–34]. This is interesting not only because entanglement generation and distribution is a fundamental primitive for quantum information science, but also because of the relevance of such states in e.g. high-dimensional quantum computing [35, 36], quantum nonlocality [37–39] and various quantum information protocols [9, 40, 41].

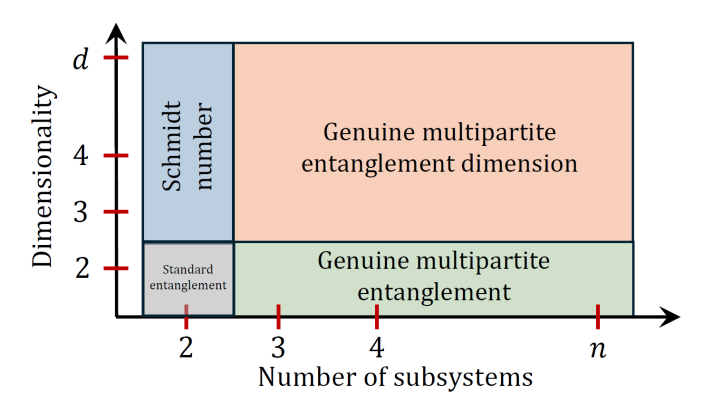


FIG. 1: **Entanglement concepts.** The Schmidt number determines the genuine dimensionality of bipartite entanglement. Genuine multipartite entanglement determines whether all *n* subsystems are entangled. The GME-dimension generalises both these concepts to systems with arbitrary dimensionality and number of subsystems.

In view of the experimental progress, it is increasingly important to conceptualise relevant notions of high-dimensional multipartite entanglement and to develop methods for benchmarking these properties in practically useful ways. To motivate the need for such concepts, it is important to note that if an n-partite system comprised of d-dimensional subsystems (qudits) is found to be GME, it does not imply that the GME truly is a d-dimensional phenomenon. Indeed, it is possible that the entanglement, albeit spread over all n qudits, can actually be simulated by using entanglement between systems with fewer than d levels. In this sense, although the system physically involves d levels, its genuine entanglement dimension is smaller.

As an illustrative example, consider a source that with probability p emits a three-qutrit Greenberger-Horne-Zeilinger (GHZ) state $\frac{1}{\sqrt{3}}\left(|000\rangle+|111\rangle+|222\rangle\right)$ and with probability 1-p emits a classical coin state $\frac{1}{3}\left(|000\rangle\langle000|+|111\rangle\langle111|+|222\rangle\langle222|\right)$. The resulting mixed state is known to be GME for every p>0 [4]. Now, let us construct a simulation that uses only entanglement

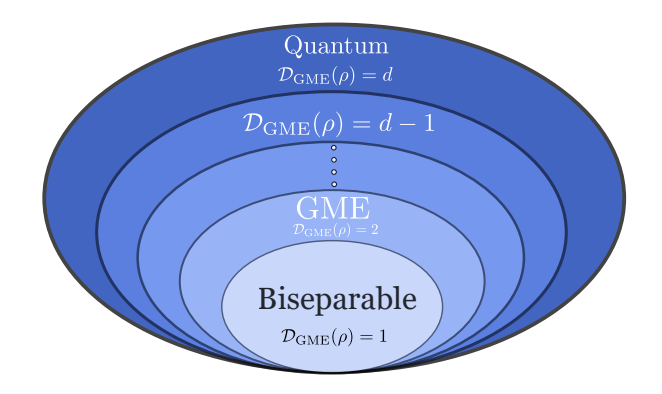


FIG. 2: **Hierarchy of GME-dimension states.** States with $\mathcal{D}_{\text{GME}}=1$ are biseparable. Any state with $\mathcal{D}_{\text{GME}}>1$ is GME, and its genuine dimension corresponds to the specific value of \mathcal{D}_{GME} . States with $\mathcal{D}_{\text{GME}}=d$ cannot be simulated by any quantum states employing a lower bipartite entanglement dimension across any bipartition of the subsystems.

between qubits. To this end, we randomly prepare one of the three different qubit GHZ states: $\frac{1}{\sqrt{2}}\left(|000\rangle+|111\rangle\right),$ $\frac{1}{\sqrt{2}}\left(|000\rangle+|222\rangle\right)$ and $\frac{1}{\sqrt{2}}\left(|111\rangle+|222\rangle\right)$. One can verify that this new mixture simulates the original source when $p=\frac{1}{2}.$ Hence, for 0 the original source has physical dimension three and is GME, but its genuine dimensionality is actually two.

The natural question is how to define the genuine dimensionality of a GME state. In contrast to bipartite states, multipartite states have no Schmidt decomposition [42], thus preventing an immediate generalisation of the Schmidt number to multipartite settings. Here, we propose to study the dimensionality of multipartite entangled systems based on ideas that naturally extend the standard concepts of GME and Schmidt number; see Figure 1. Our approach is based on a quantity that we name the GME-dimension. It admits a simple interpretation as follows. If we consider all bisections of the n systems and prepare a corresponding bipartite quantum state in each case, the GME-dimension is the smallest possible Schmidt number, respected by all these states, in order to perfectly simulate the original state via classical mixing. In other words, it is the largest bipartite entanglement dimension present in the least dimension-costly ensemble realisation of the state. In its limiting cases, where we only have two subsystems or only two levels, the GME-dimension reduces back to the Schmidt number and GME respectively (see Figure 1). The states associated with GME-dimensions ranging from 1 up to the physical dimension, d, therefore constitute a hierarchy of increasingly high-dimensional entanglement. The sets of states associated with different GME-dimensions can be pictured as a hierarchy of convex sets, as illustrated in Figure 2.

With this concept in hand, the key question is how to construct criteria for detecting the GME-dimension of arbitrary, initially uncharacterised, states. We develop three different classes of detection criteria. Firstly, we consider measuring the fidelity with a given target state and show how this implies

a bound on the GME-dimension. This generalises the standard fidelity witness method for GME [4], which is commonly used to benchmark many-qubit experiments (see e.g. [5–7, 9, 11]). While the fidelity typically does not detect a large share of relevant states [18], it has the advantages of applying to arbitrary pure target states and admitting a simple characterisation. Secondly, we develop resource-efficient detection criteria that are therefore tailored for experimental relevance. This is motivated by the fact that high-dimensional multipartite entanglement sources typically are complex, leading to limited count rates. Also, measuring the fidelity can require a lot of measurement settings, especially as d increases. Together, this can quickly become a significant obstacle for experiments. Therefore, our method allows the fidelity to be estimated using only the minimal number of measurements, namely two. We explicitly construct such minimal criteria for the two most broadly considered high-dimensional multipartite states, namely GHZ and cluster states, for any n and d. We find that the criteria perform well under realistic noise conditions. Thirdly, we employ convex programming methods to determine conditions for a state's GME-dimension. We show that this leads to considerably stronger GME-dimension criteria than what is possible with fidelity witnesses. With this type of approach, we also show that for experiments involving a few particles and a few levels, this method can offer particularly noise-tolerant detection criteria using a small number of measurement settings.

II. DIMENSIONALITY OF GENUINE MULTIPARTITE ENTANGLEMENT

The entanglement structure of quantum systems with n>2 subsystems is richer than in the bipartite case. A pure state, $|\psi\rangle$, is called k-separable if there exists a partition of the subsystems, $\mathcal{P}_k = \{S_j\}_{j=1}^k$, such that $|\psi\rangle = |\psi_1\rangle_{S_1}\otimes\ldots\otimes|\psi_k\rangle_{S_k}$. A density matrix $\rho\in\mathcal{L}(\mathcal{H}_1\otimes\cdots\otimes\mathcal{H}_n)$ is called k-separable if it is decomposable as a convex combination over pure states k-separable w.r.t some \mathcal{P}_k , i.e. $\rho=\sum_i\sum_j q_{i,j}|\psi_j\rangle\langle\psi_j|_i$, where $q_{i,j}\geq 0$ and $\sum_{i,j}q_{i,j}=1$, and the index i runs over all choices of \mathcal{P}_k . The number of partitions equals the Stirling number of the second kind, $g(n;k)=\sum_{i=1}^k (-1)^{k-i}i^{n-1}/((i-1)!(k-i)!)$. Here, the strongest entanglement is that which admits no 2-separable (biseparable) decomposition, better known as GME. Thus, GME states are impossible to generate using classical randomness and arbitrary n-partite states, each separable w.r.t some bipartition $\mathcal{P}_2=\{S,\bar{S}\}$.

In order to further develop the notion of GME so that it also addresses the dimensionality of the entanglement, we substitute the requirement of separability across each $\{S,\bar{S}\}$ in the respective elements of the ensemble decomposition with a constraint on the Schmidt number across the same bipartiton. That is, for a generic n-partite and d-dimensional density matrix ρ , we consider decompositions of the form

$$\rho = \sum_{S|\bar{S}} q_{S|\bar{S}} \sigma_{S|\bar{S}} \tag{1}$$

where the sum goes over all g(n;2) bipartitions, $\{q_{S|\bar{S}}\}$ is a probability distribution and $\sigma_{S|\bar{S}}$ is a state of local dimensions $d^{|S|}$ and $d^{|\bar{S}|}$, whose Schmidt number is no more than r. The latter limitation means that for each $\{S,\bar{S}\}$ there exists a pure-state decomposition $\sigma_{S|\bar{S}} = \sum_i p_{i,S|\bar{S}} \left| \psi_{i,S|\bar{S}} \middle| \psi_{i,S|\bar{S}} \right|$ where the largest Schmidt rank over all pure states $\{\left|\psi_{i,S|\bar{S}}\right>\}_i$ does not exceed r. In contrast, if no decomposition on the form (1) exists, the simulation of ρ via classical randomness and bipartite quantum states then requires that at least one of the ensemble states $\sigma_{S|\bar{S}}$ has a Schmidt number exceeding r. This naturally leads us to our main quantity of interest; the largest r found over all the bipartitions, in the least "expensive" ensemble realisations of ρ . We call this the GME-dimension.

Definition 1 (GME-dimension). For an arbitrary n-partite state ρ , its GME-dimension is

$$\mathcal{D}_{\text{GME}}(\rho) = \min_{\{q_{S|\bar{S}}\}, \{\sigma_{S|\bar{S}}\}} \left\{ r_{\text{max}} : \rho = \sum_{S|\bar{S}} q_{S|\bar{S}} \, \sigma_{S|\bar{S}} \right.$$

$$\text{and } r_{\text{max}} = \max_{\{S|\bar{S}\}} r_{S|\bar{S}} \right\},$$
(2)

where $r_{S|\bar{S}}$ is the Schmidt number of $\sigma_{S|\bar{S}}$ across $\{S,\bar{S}\}$.

Notably, setting n=2 reduces the GME-dimension to the Schmidt number, as there is only one possible bipartiton. Furthermore, setting $\mathcal{D}_{\text{GME}}=1$ instead reduces it to the definition of biseparability. For fixed (n,d), we write $\mathcal{G}_{d_{\text{GME}}}$ for the set of states obeying $\mathcal{D}_{\text{GME}}(\rho) \leq d_{\text{GME}}$.

A different approach to classifying high-dimensional multipartite entanglement was proposed in [43]. For pure states, it is based on computing the Schmidt rank across every bipartition and ordering them in a vector. For mixed states, the ordered vector is constructed by separately computing the Schmidt number across every bipartition. This concept is inequivalent to the GME-dimension but a connection exists for pure states. In the special case of pure states, \mathcal{D}_{GME} is the smallest Schmidt rank over all bipartitions, i.e. the smallest element of the Schmidt vector. For mixed states, this connection ceases to hold. Consider, for instance, the state

$$\rho = \frac{1}{3} \left(\phi_{AB}^+ \otimes |2\rangle\!\langle 2|_C + \phi_{BC}^+ \otimes |2\rangle\!\langle 2|_A + \phi_{AC}^+ \otimes |2\rangle\!\langle 2|_B \right) \tag{3}$$
 where $\phi^+ = |\phi^+\rangle\!\langle \phi^+|$ with $|\phi^+\rangle = \frac{1}{\sqrt{2}} \left(|00\rangle + |11\rangle \right)$ is the standard two-qubit maximally entangled state. Since the state is biseparable, it follows directly from Definition 1 that $\mathcal{D}_{\text{GME}}(\rho) = 1$. However, ρ is entangled across all bipartitions because $\rho^{T_A} \ngeq 0$, $\rho^{T_B} \ngeq 0$ and $\rho^{T_C} \ngeq 0$, which implies that all entries of the Schmidt vector are at least two and hence larger than the GME-dimension.

III. FIDELITY WITNESSES

Measuring the fidelity, $F_{\psi}(\rho) = \langle \psi | \rho | \psi \rangle$, between a pure target state ψ and a mixed lab state ρ is a standard way to detect GME in the vicinity of ψ . Therefore, we begin with iden-

tifying how the fidelity also can be used to detect the GME-dimension.

Result 1 (Fidelity witness). For any n-partite pure target state ψ with local dimension d, its fidelity with any state ρ with GME-dimension no larger than d_{GME} is bounded as

$$\max_{\rho \in \mathcal{G}_{d_{GME}}} F_{\psi}(\rho) \le \max_{\{S, \bar{S}\}} \sum_{i=1}^{d_{GME}} \lambda_i(\psi_S), \tag{4}$$

where the maximisation is over all bipartitions of the subsystems and $\lambda(\psi_S)$ is the spectrum of the reduced state $\psi_S = \operatorname{tr}_{\bar{S}}(\psi)$, ordered non-increasingly.

Proof. We show this result in two ways. A straightforward argument builds directly on extending previously known properties of the bipartite fidelity to the multipartite case. For n=2, for which there is only one bipartition, it is known that (4) holds [44]. Due to the linearity of the fidelity function and the convexity of the set $\mathcal{G}_{d_{\text{GME}}}, F_{\psi}(\rho)$ is optimised for a pure state $\rho = |\phi\rangle\langle\phi| \in \mathcal{G}_{d_{\text{GME}}}$. Thus, we may separately consider each bipartition and select the maximal value.

We also show the result without relying on the bipartite case, with the complete details given in Supplementary Material (Appendix A). Again, we use that each bipartition can be considered separately. For a given $\{S, \bar{S}\}$, we can use the monotonicity of the fidelity function [45, 46], namely that $F_{\psi}(\phi) \leq F_{\psi_S}(\phi_S) = \left(\operatorname{tr}\sqrt{\sqrt{\phi_S}\psi_S\sqrt{\phi_S}}\right)^2$. For general mixed states ψ_S , we use in SM the Lagrange multiplier method to formulate the optimisation of $F_{\psi_S}(\phi_S)$ as a linear program. It is shown that argument of the RHS of (4) is obtained at a feasible point of both the primal and dual program, and thus attains optimality because of the strong duality of linear programing.

Notice that choosing $d_{\text{GME}} = 1$ reduces Result 1 to the standard fidelity witness for GME [4].

It is important to consider Result 1 in practically relevant cases. We have evaluated it explicitly, for arbitrary choices of (n,d), for three different seminal families of states, namely GHZ states, cluster states and absolutely maximally entangled states (assuming they exist, see [47, 48]). In all three cases, the fidelity witness for the GME-dimension is identical; it reads

$$F_{\psi}(\rho) \le \frac{d_{\text{GME}}}{d},$$
 (5)

which is notably independent of n. Our proof for the former and latter state is straightforward, but less so for cluster states; see details in Appendix B. Importantly, while (5) provides a simple criterion of general validity, it also means that fidelity methods cannot distinguish between these three classes of states.

IV. MINIMAL FIDELITY WITNESSES

With multipartite high-dimensional states, it is often practically relevant to probe the system using as few measure-

ments as possible. Therefore, we now aim to detect the GME-dimension via fidelity estimation from only two complementary global product bases. This is the minimal setting for detecting the GME-dimension via fidelity estimation.

First, we target states in the vicinity of the GHZ state,

$$\left| \mathsf{ghz}_{n,d} \right\rangle = \frac{1}{\sqrt{d}} \sum_{i=0}^{d-1} \left| i \right\rangle^{\otimes n},$$
 (6)

for arbitrary (n,d). Let $\{|j\rangle\}_{j=0}^{d-1}$ be the computational basis and $\{|e_j\rangle\}_{j=0}^{d-1}$ the Fourier basis, $|e_j\rangle=\frac{1}{\sqrt{d}}\sum_{k=0}^{d-1}\omega^{jk}\,|k\rangle$, where $\omega=e^{\frac{2\pi i}{d}}$. Consider that we (i) measure all subsystems in the computational basis and compute the total probability of all n local outcomes being identical, and (ii) measure all subsystems in the Fourier basis and compute the total probability that the sum over all local outcomes is divisible by d. The Hermitian operator describing the sum of these two events takes the form

$$O_{n,d}^{\text{ghz}} = \sum_{j=0}^{d-1} |j\rangle\langle j|^{\otimes n} + \sum_{j_1,\dots,j_n=0}^{d-1} \bigotimes_{l=1}^{n} |e_{j_l}\rangle\langle e_{j_l}| \,\delta_{j_1 \oplus \dots \oplus j_n,0},$$

where \oplus denotes addition modulo d. The entanglement witness is the expectation value, $\mathcal{W}_{n,d}^{\rm ghz}(\rho)={\rm tr}\left(\rho O_{n,d}^{\rm ghz}\right).$ It is immediate that the GHZ state has perfect correlations for the event (i) and a direct calculation shows the same also for event (ii). Hence, $\mathcal{W}_{n,d}^{\rm ghz}({\rm ghz}_{n,d})=2.$ Our next result shows how this witness detects the GME-dimension.

Result 2 (Minimal GHZ state witness). For any n-partite state ρ of local dimension d with GME-dimension no larger than d_{GME} ,

$$W_{n,d}^{ghz}(\rho) \le 1 + \frac{d_{GME}}{d},\tag{8}$$

Moreover, any observed value of $W_{n,d}^{ghz}$ implies a GHZ-fidelity bound $F_{ghz}(\rho) \geq W_{n,d}^{ghz}(\rho) - 1$.

The proof is analytical and based on the insight that the witness operator (7) can be decomposed as a sum of a projector and the GHZ state. See Appendix C for details.

Naturally, since we use only two global product bases (independently of n and d), this criterion is weaker than the exact fidelity criterion, but it is practically advantageous. Importantly, it can perform well for the two most relevant noise models, namely depolarisation and dephasing. Take first depolarising (white) noise, corresponding to $\rho_v^{\rm ghz} = v \left| {\rm ghz}_{n,d} \right\rangle \left\langle {\rm ghz}_{n,d} \right| + \frac{1-v}{d^n} \mathbb{1}$, where $v \in [0,1]$ is the visibility. The critical visibility for violating inequality (8) is

$$v_{\text{crit}} = \frac{1 - d^{n-2}(d_{\text{GME}} + d - 1)}{1 - d^{n-2}(2d - 1)}.$$
 (9)

For instance, take a system of four qutrits; the threshold for detecting $d_{\rm GME}=3$ becomes $v_{\rm crit}=79.5\%$, which is around the regime relevant for state-of-the-art experiments. Next,

consider instead dephasing noise, corresponding to $\tau_v^{\rm ghz} = v \left| {\rm ghz}_{n,d} \right\rangle \left\langle {\rm ghz}_{n,d} \right| + \frac{1-v}{d} \sum_{i=0}^{d-1} |i\rangle \langle i|^{\otimes n}.$ The critical visibility from Result 2 becomes $v_{\rm crit} = \frac{d_{\rm GME}-1}{d-1}$, independently of n. We observe that this equals what is obtained from Eq. (5) by using complete fidelity measurements. In fact, we prove in Appendix D that $v_{\rm crit}$ is the exact threshold for the GME-dimension of $\tau_v^{\rm ghz}$, i.e. our minimal witness is actually necessary and sufficient.

Moreover, by using only a few more measurements, one can build witnesses with enhanced detection power. We exemplify this in Appendix $\bf E$ where we consider three-partite systems and use ten global product bases to construct a fidelity estimation witness for odd values of d.

Another important class of states are cluster states. High-dimensional cluster states are generated in lattices of n qudits with Ising-type interaction; in a linear lattice they take the form

$$|C_{n,d}\rangle = \frac{1}{\sqrt{d^n}} \bigotimes_{a=1}^n \left(\sum_{k=0}^{d-1} |k\rangle_a Z_{a+1}^k \right),$$
 (10)

with $Z = \sum_{k=1}^{d} \omega^k |k\rangle\langle k|$ and the convention $Z_{n+1} = 1$ [49]. Using only two global product bases, we construct a GME-dimension witness targeting $|C_{n,d}\rangle$.

Consider that we (i) measure the odd subsystems in the Fourier basis and the even ones in the computational basis and (ii) measure the odd subsystems in the computational basis and the even ones in the Fourier basis. The relevant outcome combinations are different from those used before for GHZ. Specifically, they correspond to the Hermitian operator,

$$\begin{split} O_{n,d}^{\text{cluster}} &= \bigotimes_{l \text{ odd }} \sum_{q_{l},p_{l+1}=0}^{d-1} |e_{q_{l}}p_{l+1}\rangle\!\langle e_{q_{l}}p_{l+1}| \, \delta_{p_{l+1} \oplus p_{l-1} \ominus q_{l},0} \\ &+ \bigotimes_{l \text{ odd }} \sum_{p_{l},q_{l+1}=0}^{d-1} \left| p_{l}e_{q_{l+1}} \middle\rangle\!\langle p_{l}e_{q_{l+1}} \right| \, \delta_{p_{l} \oplus p_{l+2} \ominus q_{l+1},0}. \end{split}$$

The total probability associated to observing these outcomes in events (i) and (ii) corresponds to the entanglement witness, i.e. $\mathcal{W}_{n,d}^{\text{cluster}}(\rho) = \operatorname{tr}\left(\rho O_{n,d}^{\text{cluster}}\right)$. The witness is constructed so that the cluster state exhibits perfect correlations for both (i) and (ii), and hence $\mathcal{W}_{n,d}^{\text{cluster}}(C_{n,d}) = 2$. The next result shows how this witness detects the GME-dimension.

Result 3 (Minimal cluster state witness). For any n-partite state ρ of local dimension d with GME-dimension no larger than d_{GME} ,

$$W_{n,d}^{cluster}(\rho) \le 1 + \frac{d_{GME}}{d}$$
 (12)

Moreover, any observed value of $W_{n,d}^{cluster}$ implies a cluster state fidelity bound $F_{cluster}(\rho) \geq W_{n,d}^{cluster}(\rho) - 1$.

The proof of this result is given in Appendix F and largely parallels the ideas used to derive Result 2.

In analogy with the previous, we apply Result 3 to cluster states with depolarising and dephasing noise, namely $\rho_v^{\text{cluster}} =$

 $v |C_{n,d}\rangle\langle C_{n,d}| + \frac{1-v}{d^n} 1$ and $\tau_v^{ ext{cluster}} = v |C_{n,d}\rangle\langle C_{n,d}| + \frac{1-v}{d} \sum_{i=0}^{d-1} |i\rangle\langle i|^{\otimes n}$, respectively. Curiously, the two critical noise thresholds turn out identical, namely

$$v_{\text{crit}} = \frac{b - d^{\frac{n}{2} + a} - d^{\frac{n}{2} + a - 1} d_{\text{GME}}}{b - 2d^{\frac{n}{2} + a}},$$
 (13)

where $b=1+d^{2a}$ and $a=(1+(-1)^{n+1})/4$. Continuing the example of four qutrits with a maximal GME-dimension, this becomes $v_{\rm crit}=81.3\%$.

V. CONVEX PROGRAMMING METHOD

It is expected that the GME-dimension of many states is not detectable using only fidelity-based criteria. Therefore, we now go further and detect the GME-dimension via convex programming relaxations [50] of the set \mathcal{G}_r . To this end, let Λ be an r-positive trace-preserving map. Such maps are positive when applied to one share of every bipartite state with Schmidt number at most r but non-positive for some states with larger Schmidt number [14]. For any r-positive map, we define the semidefinite program

$$\max_{v,\tilde{\sigma}} v$$
s.t.
$$v\rho + \frac{1-v}{d^n} \mathbb{1} = \sum_{S|\bar{S}} \tilde{\sigma}_{S|\bar{S}},$$

$$\tilde{\sigma}_{S|\bar{S}} \ge 0 \quad \forall (S|\bar{S}),$$

$$(\Lambda_S \otimes \mathbb{1}_{\bar{S}})[\tilde{\sigma}_{S|\bar{S}}] \ge 0 \quad \forall (S|\bar{S}),$$

$$(14)$$

where $\tilde{\sigma}_{S|\bar{S}}=q_{S|\bar{S}}\sigma_{S|\bar{S}}$ are unnormalised states. Here, we have chosen to introduce depolarising noise on the state ρ . This serves as one of several possible quantifiers of the robustness of ρ w.r.t. the selected relaxation of \mathcal{G}_r . Thus, obtaining any value v < 1 implies that $\rho \notin \mathcal{G}_r$ and hence $\mathcal{D}_{GME}(\rho) > r$. For example, selecting Λ as the partial transpose map, which is 1-positive, reduces Eq. (14) to the approach first outlined in Ref. [51] for detecting standard GME. This partial transpose map can be adapted for our higher-dimensional analysis by introducing auxiliary Hilbert spaces of dimension r for each qudit [16]. However, the extra dimensions accumulate exponentially in n when r > 1, causing a large computational overhead. Therefore, we instead propose to use the generalised reduction map, $\Lambda(X) = \operatorname{tr} X \mathbb{1} - \alpha X$, which is r-positive when $\alpha = \frac{1}{\pi}$ [14, 52]. Note that applying the map on the system S, as in Eq. (14), is not necessarily equivalent to applying it on system S. They correspond to different relaxations, and one can even apply it to both subsystems separately to obtain a more accurate relaxation of \mathcal{G}_r .

If ρ is a pure state (e.g. the GHZ state or the cluster state) and we use the generalised reduction map, the semidefinite program (14) can be reduced to a linear program. This speeds up computations. To achieve this, one chooses any basis $\{|\psi_i\rangle\}_{i=1}^{d^n}$ where the first element is the target state, $|\psi_1\rangle\langle\psi_1|=\rho$. As shown in Appendix G, the linear program is obtained by representing (14) in this state-diagonal basis. If ρ

(n,d)	$\mathcal{D}_{ ext{GME}}(ho)$	v _{ghz} (LP)	v _{cluster} (LP)	v (fidelity)
(3,3)	1	0.2500	*	0.3077
(3,3)	2	0.5909	*	0.6538
(4,3)	1	0.2203	0.2174	0.3250
(4,3)	2	0.6029	0.5129	0.6625
(4,4)	3	0.6503	0.534	0.7490

TABLE I: Critical visibility, v, from convex programming relaxation for the GME-dimension. Case study presented for target GHZ states and cluster states under white noise. Note that these states are local-unitary equivalent for n=3. The results are compared with the fidelity bound (5).

is a graph state, similar reductions are possible also for standard GME tests based on the partial transpose map [53]. One may further notice that depending on the choice of pure state ρ , additional symmetries may be available, permitting further reductions of the linear program. For instance, for the GHZ state, one can also exploit the invariance under permutations of subsystems. This allows one to reduce from g(n; 2) diagonal matrices to just n-1 diagonal matrices in the optimisation.

We have evaluated both the semidefinite program (14) and the corresponding linear program. Notably, the dual program provides an explicit witness for the GME-dimension. On a standard computer, we could efficiently evaluate the linear program up to e.g. (n,d)=(5,4) for the GHZ state and (n,d)=(4,4) for the cluster state. Our implementation is available at [54]. In Table I we display some of the resulting bounds on the critical visibility; more extensive results are given in Appendix H. The key observation is that the visibilities are significantly smaller than those obtained from the fidelity witness (5). This showcases the conceptual relevance of this method. It is also practically relevant since most experiments presently concern choices of (n,d>2) [28–34] that are efficiently computable with this method.

Furthermore, this method can also be used to give resource-efficient criteria beyond fidelity estimation. This is particularly natural for experimental considerations, where both noise and coincidence rates can be a significant challenge. With this aim, we no longer want to simulate the whole state ρ , but only its statistics when a small number of measurements are performed on it. For this, we can choose any set of global product projections $\{M_i\}$ and bound the white noise tolerance by evaluating the SDP

$$\max_{v,\tilde{\sigma}} v$$
s.t.
$$\operatorname{tr}\left(\left(v\rho + \frac{1-v}{d^n}\mathbb{1}\right)M_i\right) = \operatorname{tr}\left(\sum_{S|\bar{S}}\tilde{\sigma}_{S|\bar{S}}M_i\right) \,\forall i,$$

$$\tilde{\sigma}_{S|\bar{S}} \geq 0 \quad \forall (S|\bar{S}),$$

$$(\Lambda_S \otimes \mathbb{1}_{\bar{S}})[\tilde{\sigma}_{S|\bar{S}}] \geq 0 \quad \forall (S|\bar{S}).$$
(15)

To showcase this method, we consider that $\{M_i\}$ corresponds to just two or three global product measurements, in which all local measurements are mutually unbiased bases (MUBs)

(n,d)	$\mathcal{D}_{ ext{GME}}(ho)$	v (fidelity)	v (min fid)	v (2 MUB)	v (3 MUB)
(3,3)	2	0.6538	0.7857	0.7500	0.6667
(3,4)	3	0.7460	0.8518	0.8222	0.7576
(4,3)	2	0.6625	0.7954	0.7750	0.7097

TABLE II: Comparison between values of critical visibility, v, for different GME-dimensions obtained from: fidelity criterion (5), minimal fidelity witness (9), convex programming relaxations (15) based on simulating statistics from two and three global product measurements. Case study presented for target GHZ states under white noise.

[55]. The results are displayed in Table II based on the GHZ state and a maximal GME-dimension. We see that using two MUBs (the computational basis and the Fourier basis) improves on the minimal fidelity witnesses previously derived. Note that the measurements in both cases are identical. More significantly, we also see that just performing one additional global product measurement of a suitable MUB, the noise tolerance significantly improves.

VI. CONCLUSIONS

We have proposed the GME-dimension as a generalisation of the standard concepts of GME and Schmidt number in order to benchmark genuinely high-dimensional forms of multipartite entanglement. We developed several different types of criteria for detecting the GME-dimension: (i) the fidelity, which is generally applicable to arbitrary target states, (ii) the minimal fidelity witnesses, which are relevant for resource-efficiency in experiments targeting the seminal GHZ and cluster states, and (iii) the convex programming criteria, which reveal significantly better noise tolerance than fidelity witnesses. These methods can readily be applied to experiments concerned with generating high-dimensional multipartite entanglement.

It is an interesting open problem how much noise various states tolerate before their GME-dimension is reduced. Furthermore, it is well-known that high-dimensional GME can persist under diverging noise rates [56–58] but it is an open problem whether anything similar is possible for larger, or even maximal, GME-dimension. Connected to this is also the question of which classes of states that are most strongly entangled in the GME-dimension sense. For instance, Table I already suggests that the cluster state is more strongly high-dimensionally GME than the GHZ state. From this point of view, there may be even more interesting high-dimensional multipartite states to study.

ACKNOWLEDGMENTS

We thank Otfried Gühne for useful comments and Emmanuel Zambrini Cruzeiro for computation support. This work is supported by the Wenner-Gren Foundation and by the Knut and Alice Wallenberg Foundation through the Wallenberg Center for Quantum Technology (WACQT).

- [1] R. Horodecki, P. Horodecki, M. Horodecki, and K. Horodecki, Quantum entanglement, Rev. Mod. Phys. 81, 865 (2009).
- [2] M. Seevinck and J. Uffink, Sufficient conditions for threeparticle entanglement and their tests in recent experiments, Phys. Rev. A 65, 012107 (2001).
- [3] O. Gühne and G. Tóth, Entanglement detection, Physics Reports 474, 1 (2009).
- [4] M. Bourennane, M. Eibl, C. Kurtsiefer, S. Gaertner, H. Weinfurter, O. Gühne, P. Hyllus, D. Bruß, M. Lewenstein, and A. Sanpera, Experimental detection of multipartite entanglement using witness operators, Physical Review Letters 92, 10.1103/physrevlett.92.087902 (2004).
- [5] H. Häffner, W. Hänsel, C. F. Roos, J. Benhelm, D. Chek-al kar, M. Chwalla, T. Körber, U. D. Rapol, M. Riebe, P. O. Schmidt, C. Becher, O. Gühne, W. Dür, and R. Blatt, Scalable multiparticle entanglement of trapped ions, Nature 438, 643 (2005).
- [6] C.-Y. Lu, X.-Q. Zhou, O. Gühne, W.-B. Gao, J. Zhang, Z.-S. Yuan, A. Goebel, T. Yang, and J.-W. Pan, Experimental entanglement of six photons in graph states, Nature Physics 3, 91 (2007).
- [7] W.-B. Gao, C.-Y. Lu, X.-C. Yao, P. Xu, O. Gühne, A. Goebel, Y.-A. Chen, C.-Z. Peng, Z.-B. Chen, and J.-W. Pan, Experimental demonstration of a hyper-entangled ten-qubit schrödinger cat state, Nature Physics 6, 331 (2010).
- [8] X.-C. Yao, T.-X. Wang, P. Xu, H. Lu, G.-S. Pan, X.-H. Bao, C.-Z. Peng, C.-Y. Lu, Y.-A. Chen, and J.-W. Pan, Observation of eight-photon entanglement, Nature Photonics 6, 225 (2012).

- [9] X.-L. Wang, L.-K. Chen, W. Li, H.-L. Huang, C. Liu, C. Chen, Y.-H. Luo, Z.-E. Su, D. Wu, Z.-D. Li, H. Lu, Y. Hu, X. Jiang, C.-Z. Peng, L. Li, N.-L. Liu, Y.-A. Chen, C.-Y. Lu, and J.-W. Pan, Experimental ten-photon entanglement, Phys. Rev. Lett. 117, 210502 (2016).
- [10] H.-S. Zhong, Y. Li, W. Li, L.-C. Peng, Z.-E. Su, Y. Hu, Y.-M. He, X. Ding, W. Zhang, H. Li, L. Zhang, Z. Wang, L. You, X.-L. Wang, X. Jiang, L. Li, Y.-A. Chen, N.-L. Liu, C.-Y. Lu, and J.-W. Pan, 12-photon entanglement and scalable scattershot boson sampling with optimal entangled-photon pairs from parametric down-conversion, Phys. Rev. Lett. 121, 250505 (2018).
- [11] P. Thomas, L. Ruscio, O. Morin, and G. Rempe, Efficient generation of entangled multiphoton graph states from a single atom, Nature 608, 677 (2022).
- [12] N. Friis, G. Vitagliano, M. Malik, and M. Huber, Entanglement certification from theory to experiment, Nature Reviews Physics 1, 72 (2019).
- [13] M. Erhard, M. Krenn, and A. Zeilinger, Advances in highdimensional quantum entanglement, Nature Reviews Physics 2, 365 (2020).
- [14] B. M. Terhal and P. Horodecki, Schmidt number for density matrices, Physical Review A 61, 10.1103/physreva.61.040301 (2000).
- [15] A. Sanpera, D. Bruß, and M. Lewenstein, Schmidt-number witnesses and bound entanglement, Phys. Rev. A 63, 050301 (2001).
- [16] F. Hulpke, D. Bruss, M. Lewenstein, and A. Sanpera, Simpli-

- fying Schmidt number witnesses via higher-dimensional embeddings, Quantum Inf. Comput. **4**, 207 (2004), arXiv:quant-ph/0401118.
- [17] F. Shahandeh, J. Sperling, and W. Vogel, Operational gaussian schmidt-number witnesses, Phys. Rev. A 88, 062323 (2013).
- [18] M. Weilenmann, B. Dive, D. Trillo, E. A. Aguilar, and M. Navascués, Entanglement detection beyond measuring fidelities, Phys. Rev. Lett. 124, 200502 (2020).
- [19] N. Wyderka, G. Chesi, H. Kampermann, C. Macchiavello, and D. Bruß, Construction of efficient schmidt-number witnesses for high-dimensional quantum states, Phys. Rev. A 107, 022431 (2023).
- [20] S. Morelli, M. Huber, and A. Tavakoli, Resource-efficient highdimensional entanglement detection via symmetric projections, Phys. Rev. Lett. 131, 170201 (2023).
- [21] A. Tavakoli and S. Morelli, Enhanced schmidt number criteria based on correlation trace norms (2024), arXiv:2402.09972 [quant-ph].
- [22] A. C. Dada, J. Leach, G. S. Buller, M. J. Padgett, and E. Andersson, Experimental high-dimensional two-photon entanglement and violations of generalized bell inequalities, Nature Physics 7, 677 (2011).
- [23] M. Krenn, M. Huber, R. Fickler, R. Lapkiewicz, S. Ramelow, and A. Zeilinger, Generation and confirmation of a (100 × 100)-dimensional entangled quantum system, Proceedings of the National Academy of Sciences 111, 6243 (2014), https://www.pnas.org/doi/pdf/10.1073/pnas.1402365111.
- [24] J. Bavaresco, N. Herrera Valencia, C. Klöckl, M. Pivoluska, P. Erker, N. Friis, M. Malik, and M. Huber, Measurements in two bases are sufficient for certifying high-dimensional entanglement, Nature Physics 14, 1032 (2018).
- [25] N. Herrera Valencia, V. Srivastav, M. Pivoluska, M. Huber, N. Friis, W. McCutcheon, and M. Malik, High-Dimensional Pixel Entanglement: Efficient Generation and Certification, Quantum 4, 376 (2020).
- [26] S. Designolle, V. Srivastav, R. Uola, N. H. Valencia, W. McCutcheon, M. Malik, and N. Brunner, Genuine highdimensional quantum steering, Phys. Rev. Lett. 126, 200404 (2021).
- [27] S. Goel, S. Leedumrongwatthanakun, N. H. Valencia, W. Mc-Cutcheon, A. Tavakoli, C. Conti, P. W. H. Pinkse, and M. Malik, Inverse design of high-dimensional quantum optical circuits in a complex medium, Nature Physics 20, 232 (2024).
- [28] M. Malik, M. Erhard, M. Huber, M. Krenn, R. Fickler, and A. Zeilinger, Multi-photon entanglement in high dimensions, Nature Photonics 10, 248 (2016).
- [29] M. Erhard, M. Malik, M. Krenn, and A. Zeilinger, Experimental greenberger-horne-zeilinger entanglement beyond qubits, Nature Photonics 12, 759 (2018).
- [30] P. Imany, J. A. Jaramillo-Villegas, M. S. Alshaykh, J. M. Lukens, O. D. Odele, A. J. Moore, D. E. Leaird, M. Qi, and A. M. Weiner, High-dimensional optical quantum logic in large operational spaces, npj Quantum Information 5, 59 (2019).
- [31] C. Reimer, S. Sciara, P. Roztocki, M. Islam, L. Romero Cortés, Y. Zhang, B. Fischer, S. Loranger, R. Kashyap, A. Cino, S. T. Chu, B. E. Little, D. J. Moss, L. Caspani, W. J. Munro, J. Azaña, M. Kues, and R. Morandotti, High-dimensional one-way quantum processing implemented on d-level cluster states, Nature Physics 15, 148 (2019).
- [32] A. Cervera-Lierta, M. Krenn, A. Aspuru-Guzik, and A. Galda, Experimental high-dimensional greenberger-horne-zeilinger entanglement with superconducting transmon qutrits, Phys. Rev. Appl. 17, 024062 (2022).
- [33] J. Bao, Z. Fu, T. Pramanik, J. Mao, Y. Chi, Y. Cao, C. Zhai,

- Y. Mao, T. Dai, X. Chen, X. Jia, L. Zhao, Y. Zheng, B. Tang, Z. Li, J. Luo, W. Wang, Y. Yang, Y. Peng, D. Liu, D. Dai, Q. He, A. L. Muthali, L. K. Oxenløwe, C. Vigliar, S. Paesani, H. Hou, R. Santagati, J. W. Silverstone, A. Laing, M. G. Thompson, J. L. O'Brien, Y. Ding, Q. Gong, and J. Wang, Very-large-scale integrated quantum graph photonics, Nature Photonics 17, 573 (2023).
- [34] W.-B. Xing, X.-M. Hu, Y. Guo, B.-H. Liu, C.-F. Li, and G.-C. Guo, Preparation of multiphoton high-dimensional ghz states, Opt. Express 31, 24887 (2023).
- [35] Y. Chi, J. Huang, Z. Zhang, J. Mao, Z. Zhou, X. Chen, C. Zhai, J. Bao, T. Dai, H. Yuan, M. Zhang, D. Dai, B. Tang, Y. Yang, Z. Li, Y. Ding, L. K. Oxenløwe, M. G. Thompson, J. L. O'Brien, Y. Li, Q. Gong, and J. Wang, A programmable qudit-based quantum processor, Nature Communications 13, 1166 (2022).
- [36] M. Ringbauer, M. Meth, L. Postler, R. Stricker, R. Blatt, P. Schindler, and T. Monz, A universal qudit quantum processor with trapped ions, Nature Physics 18, 1053 (2022).
- [37] N. J. Cerf, S. Massar, and S. Pironio, Greenberger-hornezeilinger paradoxes for many qudits, Phys. Rev. Lett. 89, 080402 (2002).
- [38] W. Tang, S. Yu, and C. H. Oh, Greenberger-horne-zeilinger paradoxes from qudit graph states, Phys. Rev. Lett. 110, 100403 (2013).
- [39] R. Augusiak, A. Salavrakos, J. Tura, and A. Acín, Bell inequalities tailored to the greenberger–horne–zeilinger states of arbitrary local dimension, New Journal of Physics 21, 113001 (2019).
- [40] M. Fitzi, N. Gisin, and U. Maurer, Quantum solution to the byzantine agreement problem, Phys. Rev. Lett. 87, 217901 (2001).
- [41] A. Cabello, *n*-particle *n*-level singlet states: Some properties and applications, Phys. Rev. Lett. **89**, 100402 (2002).
- [42] N. Linden, S. Popescu, and S. Popescu, On multi-particle entanglement, Fortschritte der Physik 46, 567–578 (1998).
- [43] M. Huber and J. I. de Vicente, Structure of multidimensional entanglement in multipartite systems, Phys. Rev. Lett. 110, 030501 (2013).
- [44] R. Fickler, R. Lapkiewicz, M. Huber, M. P. Lavery, M. J. Padgett, and A. Zeilinger, Interface between path and orbital angular momentum entanglement for high-dimensional photonic quantum information, Nature Communications 5, 10.1038/ncomms5502 (2014).
- [45] H. Barnum, C. M. Caves, C. A. Fuchs, R. Jozsa, and B. Schumacher, Noncommuting mixed states cannot be broadcast, Physical Review Letters 76, 2818–2821 (1996).
- [46] J. Preskill, Lecture notes for physics 229: Quantum information and computation (1998).
- [47] F. Huber, C. Eltschka, J. Siewert, and O. Gühne, Bounds on absolutely maximally entangled states from shadow inequalities, and the quantum macwilliams identity, Journal of Physics A: Mathematical and Theoretical 51, 175301 (2018).
- [48] F. Huber and N. Wyderka, Table of ame states, http://www.tp.nt.uni-siegen.de/+fhuber/ame.html [Accessed: (Use the date of access)].
- [49] D. L. Zhou, B. Zeng, Z. Xu, and C. P. Sun, Quantum computation based on d-level cluster state, Phys. Rev. A 68, 062303 (2003).
- [50] A. Tavakoli, A. Pozas-Kerstjens, P. Brown, and M. Araújo, Semidefinite programming relaxations for quantum correlations (2023), arXiv:2307.02551 [quant-ph].
- [51] B. Jungnitsch, T. Moroder, and O. Gühne, Taming multiparticle entanglement, Phys. Rev. Lett. 106, 190502 (2011).

- [52] J. Tomiyama, On the geometry of positive maps in matrix algebras. ii, Linear Algebra and its Applications **69**, 169 (1985).
- [53] B. Jungnitsch, T. Moroder, and O. Gühne, Entanglement witnesses for graph states: General theory and examples, Physical Review A 84, 10.1103/physreva.84.032310 (2011).
- [54] https://github.com/GabrieleCobucci/ GMEN-mixer.git.
- [55] T. Durt, B.-G. Englert, I. Bengtsson, and K. Życzkowski, On mutually unbiased bases, International Journal of Quantum Information 08, 535–640 (2010).
- [56] M. Huber, F. Mintert, A. Gabriel, and B. C. Hiesmayr, Detection of high-dimensional genuine multipartite entanglement of mixed states, Physical Review Letters 104, 10.1103/physrevlett.104.210501 (2010).
- [57] T. Gao and Y. Hong, Separability criteria for several classes of n-partite quantum states, The European Physical Journal D 61, 765 (2011).

- [58] N. Ananth, V. K. Chandrasekar, and M. Senthilvelan, Criteria for non-k-separability of n-partite quantum states, The European Physical Journal D 69, 56 (2015).
- [59] I. Bengtsson and K. Zyczkowski, Geometry of Quantum States: An Introduction to Quantum Entanglement (Cambridge University Press, 2006).
- [60] D. P. Bertsekas, Constrained Optimization and Lagrange Multiplier Methods (Optimization and Neural Computation Series), 1st ed. (Athena Scientific, 1996).
- [61] J. Matouek and B. Gärtner, *Understanding and Using Linear Programming (Universitext)* (Springer-Verlag, Berlin, Heidelberg, 2006).
- [62] P. Skrzypczyk and D. Cavalcanti, Semidefinite Programming in Quantum Information Science, 2053-2563 (IOP Publishing, 2023).

Appendix A: Proof of the fidelity bound for GME-D

We show a linear programming based proof of *Result* 1. For clarity, we organise it in different steps:

· Convexity argument

The starting point is to note that, because of the *convexity* of the set of quantum states [59], the following inequality holds:

$$\max_{\rho: \mathcal{D}_{\text{GME}}(\rho) = d} F(\rho, \psi) \le \max_{\phi: \mathcal{D}_{\text{GME}}(\phi) = d} F(\phi, \psi), \tag{A1}$$

where ϕ is a generic *n*-partite pure state with $\mathcal{D}_{GME}(\phi) = d$.

• Monotonicity of fidelity

Since $\mathcal{D}_{\text{GME}}(\psi) = D$ and $\mathcal{D}_{\text{GME}}(\phi) = d$, for what follows from *Definition* 1 of the GME-Dimension, it is possible to find a bipartition $\alpha_2^* = (S|\bar{S})$ of the set $\{1, \ldots, n\}$ for which:

$$\psi = \sum_{k=1}^{D} \lambda_k |\lambda_k\rangle_S |\lambda'_k\rangle_{\bar{S}|S} \langle \lambda_k|_{\bar{S}} \langle \lambda'_k|, \quad \phi = \sum_{j=1}^{d} \mu_j |\mu_j\rangle_S |\mu'_j\rangle_{\bar{S}|S} \langle \mu_j|_{\bar{S}} \langle \mu'_j|, \tag{A2}$$

where $\sum_{k=1}^{D} \lambda_k = \sum_{j=1}^{d} \mu_j = 1$ and the states $\{|\lambda_k\rangle\}$, $\{|\lambda_k'\rangle\}$, $\{|\mu_j\rangle\}$, $\{|\mu_j\rangle\}$ form four orthogonal sets. Therefore, the reduction over one of the subsystems can be written as:

$$\psi^{S} = \sum_{k=1}^{D} \lambda_{k} |\lambda_{k}\rangle \langle \lambda_{k}|, \qquad \phi^{S} = \sum_{j=1}^{d} \mu_{j} |\mu_{j}\rangle \langle \mu_{j}|, \tag{A3}$$

where for simplicity we have removed the subsystem index from the braket notation.

Then, from the *monotonicity of fidelity* [45, 46], we can derive that:

$$F(\phi, \psi) \le F(\phi^S, \psi^S). \tag{A4}$$

· Symmetry and trace inequality

Now we can maximize the RHS of the inequality (A4) by starting from the definition of fidelity and its symmetry:

$$F\left(\phi^{S}, \psi^{S}\right) = \left(\operatorname{Tr}\left[\sqrt{\sqrt{\phi^{S}}\psi^{S}\sqrt{\phi^{S}}}\right]\right)^{2} = F\left(\psi^{S}, \phi^{S}\right) = \left(\operatorname{Tr}\left[\sqrt{\sqrt{\psi^{S}}\phi^{S}\sqrt{\psi^{S}}}\right]\right)^{2}.$$
 (A5)

Let's insert the decompositions showed in (A3):

$$F\left(\phi^{S}, \psi^{S}\right) = \left(\operatorname{Tr}\left[\sqrt{\sum_{k=1}^{D} \lambda_{k} \left|\lambda_{k}\right\rangle \left\langle\lambda_{k}\right| \sum_{j=1}^{d} \mu_{j} \left|\mu_{j}\right\rangle \left\langle\mu_{j}\right| \sqrt{\sum_{k'=1}^{D} \lambda_{k'} \left|\lambda_{k'}\right\rangle \left\langle\lambda_{k'}\right|}}\right]^{2}.$$
(A6)

Since the states $\{|\lambda_k\rangle\}$ and $\{|\mu_i\rangle\}$ form two orthogonal sets, we can write:

$$\sqrt{\sum_{k=1}^{D} \lambda_{k} |\lambda_{k}\rangle \langle \lambda_{k}|} = \sum_{k=1}^{D} \sqrt{\lambda_{k}} |\lambda_{k}\rangle \langle \lambda_{k}|, \qquad \sqrt{\sum_{j=1}^{d} \mu_{j} |\mu_{j}\rangle \langle \mu_{j}|} = \sum_{j=1}^{d} \sqrt{\mu_{j}} |\mu_{j}\rangle \langle \mu_{j}|, \tag{A7}$$

from which we find:

$$F(\phi^{S}, \psi^{S}) = \left(\operatorname{Tr} \left[\sqrt{\sum_{k=1}^{D} \sqrt{\lambda_{k}} |\lambda_{k}\rangle \langle \lambda_{k}| \sum_{j=1}^{d} \mu_{j} |\mu_{j}\rangle \langle \mu_{j}| \sum_{k'=1}^{D} \sqrt{\lambda_{k'}} |\lambda_{k'}\rangle \langle \lambda_{k'}|} \right] \right)^{2}$$

$$= \left(\operatorname{Tr} \left[\sqrt{\sum_{j=1}^{d} \mu_{j} \sum_{k,k'=1}^{D} \sqrt{\lambda_{k}\lambda_{k'}} |\lambda_{k}\rangle \langle \lambda_{k}|\mu_{j}\rangle \langle \mu_{j}|\lambda_{k'}\rangle \langle \lambda_{k'}|} \right] \right)^{2}.$$
(A8)

Now we can define the following non-normalized states:

$$\left\{ \left| \tilde{v}_{j} \right\rangle : \quad \left| \tilde{v}_{j} \right\rangle = \sum_{k=1}^{D} \sqrt{\lambda_{k}} \left\langle \lambda_{k} \middle| \mu_{j} \right\rangle \middle| \lambda_{k} \right\rangle, \quad j = 1, \dots, d \right\}, \tag{A9}$$

and use them in (A8) to get:

$$F\left(\phi^{S}, \psi^{S}\right) = \left(\operatorname{Tr}\left[\sqrt{\sum_{j=1}^{d} \mu_{j} \left|\tilde{v}_{j}\right\rangle \left\langle \tilde{v}_{j}\right|}\right]\right)^{2} \leq \left(\operatorname{Tr}\left[\sum_{j=1}^{d} \sqrt{\mu_{j} \left|\tilde{v}_{j}\right\rangle \left\langle \tilde{v}_{j}\right|}\right]\right)^{2},\tag{A10}$$

where in the last inequality we have used that for a set of *positive semidefinite* operators $A_i \ge 0$, the following holds¹:

$$\operatorname{Tr}\left[\sqrt{\sum_{i} A_{i}}\right] \leq \operatorname{Tr}\left[\sum_{i} \sqrt{A_{i}}\right].$$
 (A14)

Since the trace will affect just the operators, we can write:

$$\left(\operatorname{Tr}\left[\sum_{j=1}^{d} \sqrt{\mu_{j} \left|\tilde{v}_{j}\right\rangle \left\langle \tilde{v}_{j}\right|}\right]\right)^{2} = \left(\sum_{j=1}^{d} \sqrt{\mu_{j}} \operatorname{Tr} \sqrt{\left|\tilde{v}_{j}\right\rangle \left\langle \tilde{v}_{j}\right|}\right)^{2}.$$
(A15)

Then, by normalizing the states defined in (A9), we can realize that:

$$|v_{j}\rangle := \frac{|\tilde{v}_{j}\rangle}{\sqrt{\langle \tilde{v}_{j}|\tilde{v}_{j}\rangle}} \Longrightarrow \sqrt{|\tilde{v}_{j}\rangle\langle \tilde{v}_{j}|} = \sqrt{\langle \tilde{v}_{j}|\tilde{v}_{j}\rangle} |v_{j}\rangle\langle v_{j}|, \tag{A16}$$

from which we can derive that:

$$\left(\sum_{j=1}^{d} \sqrt{\mu_j} \operatorname{Tr} \sqrt{|\tilde{v}_j\rangle \langle \tilde{v}_j|}\right)^2 = \left(\sum_{j=1}^{d} \sqrt{\mu_j \langle \tilde{v}_j|\tilde{v}_j\rangle} \operatorname{Tr} \left[|v_j\rangle \langle v_j|\right]\right)^2 = \left(\sum_{j=1}^{d} \sqrt{\mu_j \langle \tilde{v}_j|\tilde{v}_j\rangle}\right)^2. \tag{A17}$$

Again, by using the definition (A9), we can find:

$$\langle \tilde{v}_j | \tilde{v}_j \rangle = \sum_{k=1}^D \lambda_k |\langle \lambda_k | \mu_j \rangle|^2, \tag{A18}$$

and therefore we can maximize (A10) as:

$$F(\phi^S, \psi^S) \le \left(\sum_{j=1}^d \sqrt{\mu_j} \sqrt{\sum_{k=1}^D \lambda_k |\langle \lambda_k | \mu_j \rangle|^2}\right)^2. \tag{A19}$$

$$\operatorname{Tr}\left[(A+B)^{\frac{1}{2}}\right]$$

$$=\operatorname{Tr}\left[(A+B)^{-\frac{1}{4}}(A+B)(A+B)^{-\frac{1}{4}}\right]$$

$$=\operatorname{Tr}\left[(A+B)^{-\frac{1}{4}}A(A+B)^{-\frac{1}{4}}\right] + \operatorname{Tr}\left[(A+B)^{-\frac{1}{4}}B(A+B)^{-\frac{1}{4}}\right],$$
(A11)

where in the last equality we have used the linearity of the trace. Now we

can use ciclicity to write:

$$\operatorname{Tr}\left[(A+B)^{-\frac{1}{4}}A(A+B)^{-\frac{1}{4}}\right] + \operatorname{Tr}\left[(A+B)^{-\frac{1}{4}}B(A+B)^{-\frac{1}{4}}\right]$$

$$= \operatorname{Tr}\left[(A+B)^{-\frac{1}{2}}A\right] + \operatorname{Tr}\left[(A+B)^{-\frac{1}{2}}B\right]$$

$$= \operatorname{Tr}\left[A^{\frac{1}{2}}(A+B)^{-\frac{1}{2}}A^{\frac{1}{2}}\right] + \operatorname{Tr}\left[B^{\frac{1}{2}}(A+B)^{-\frac{1}{2}}B^{\frac{1}{2}}\right].$$
(A12)

Then, by using that $A \leq A + B$ and $B \leq A + B$, we get:

$$\operatorname{Tr}\left[\sqrt{A+B}\right] \le \operatorname{Tr}\left[\sqrt{A} + \sqrt{B}\right].$$
 (A13)

¹ For simplicity we can prove this inequality in the case of only two operators $A \ge 0$ and $B \ge 0$. We can write:

• Lagrange multipliers method $-\mu_j$ variables

Now we can define $P_k^j := |\langle \lambda_k | \mu_j \rangle|^2$ and focus on maximizing the RHS of (A19). Since the power function is monotone, we can actually just look at its argument. Therefore, the maximization problem can be rewritten as:

$$\max_{\mu_{j},P_{k}^{j}} f(\mu_{j},P_{k}^{j}) = \max_{\mu_{j},P_{k}^{j}} \left[\sum_{j=1}^{d} \sqrt{\mu_{j}} \sqrt{\sum_{k=1}^{D} \lambda_{k} P_{k}^{j}} \right] \qquad s.t. \qquad \begin{cases} \sum_{j=1}^{d} \mu_{j} = 1, \\ P_{k}^{j} \geq 0, \\ \sum_{k=1}^{D} P_{k}^{j} = 1, \\ \sum_{k=1}^{d} P_{k}^{j} \leq 1. \end{cases}$$
raints we can notice that μ_{j} and P_{k}^{j} are independent variables. Therefore, we can start maximizing the ith respect to μ_{i} . We can use the method of $Lagrange\ multipliers\ [60]$ by defining the following constraint:

From the constraints we can notice that μ_j and P_k^j are independent variables. Therefore, we can start maximizing the function just with respect to μ_j . We can use the method of Lagrange multipliers [60] by defining the following constraint:

$$g(\mu_j) := \sum_{j=1}^d \mu_j = 1,$$
 (A21)

and by finding the solution of the following set of equations:

$$\nabla f(\mu_j, P_k^j) = \gamma \nabla g(\mu_j), \qquad \forall j = 1, \dots, d.$$
(A22)

For the generic μ_l we get:

$$\begin{cases}
\frac{\partial}{\partial \mu_l} f(\mu_j, P_k^j) = \frac{\sqrt{\sum_{k=1}^D \lambda_k P_k^j}}{2\sqrt{\mu_l}}, \\
\frac{\partial}{\partial \mu_l} g(\mu_j) = \gamma.
\end{cases}$$
(A23)

Since the RHS of (A22) results to be the same for any j, we can conclude that the values $\{\mu_j^{max}\}$ that solve the problem (A20) satisfy:

$$\sqrt{\frac{\sum_{k=1}^{D} \lambda_k P_k^1}{2\mu_1^{max}}} = \dots = \sqrt{\frac{\sum_{k=1}^{D} \lambda_k P_k^d}{2\mu_d^{max}}}.$$
 (A24)

Therefore, for two generic i, j we find:

$$\frac{\mu_i^{max}}{\frac{D}{D}} = \frac{\mu_j^{max}}{\frac{D}{D}} \implies \frac{\mu_i^{max}}{\mu_j^{max}} = \frac{\sum_{k=1}^{D} \lambda_k P_k^i}{\sum_{k=1}^{D} \lambda_k P_k^j}.$$
(A25)

We can sum both sides of the equation for i = 1, ..., d and use the constraint on the $\{\mu_i\}$ variables in (A20) to get:

$$\sum_{i=1}^{d} \frac{\mu_i^{max}}{\mu_j^{max}} = \sum_{i=1}^{d} \frac{\sum_{k=1}^{D} \lambda_k P_k^i}{\sum_{k=1}^{D} \lambda_k P_k^j} \implies \frac{1}{\mu_j^{max}} = \sum_{i=1}^{d} \frac{\sum_{k=1}^{D} \lambda_k P_k^i}{\sum_{k=1}^{D} \lambda_k P_k^j},$$
(A26)

from which we find:

$$\mu_j^{max} = \frac{\sum_{k=1}^{D} \lambda_k P_k^j}{\sum_{i=1}^{d} \sum_{k=1}^{D} \lambda_k P_k^i}.$$
(A27)

• Duality theorem $-P_k^j$ variables

We can substitute the maximum value μ_j^{max} into (A20) and focus now on the maximization with respect to the other variables P_k^j . The new problem becomes:

$$\max_{P_k^j} \sqrt{\sum_{j=1}^d \sum_{k=1}^D \lambda_k P_k^j} = \sqrt{\max_{P_k^j} \sum_{j=1}^d \sum_{k=1}^D \lambda_k P_k^j} \quad s.t. \quad \begin{cases} P_k^j \ge 0, \\ \sum_{k=1}^D P_k^j = 1, \\ \sum_{j=1}^d P_k^j \le 1. \end{cases}$$
(A28)

where, since the square root is a monotonic map, we can just focus on the maximization of its argument. In order to solve the problem we can write that:

$$\sum_{j=1}^{d} \sum_{k=1}^{D} \lambda_k P_k^j = \sum_{k=1}^{D-1} \sum_{j=1}^{d} \lambda_k P_k^j + \lambda_D \sum_{j=1}^{d} \left(1 - \sum_{l=1}^{D-1} P_l^j \right) = \sum_{k=1}^{D-1} \sum_{j=1}^{d} (\lambda_k - \lambda_D) P_k^j + d\lambda_D, \tag{A29}$$

where we have used the second constraint in (A28). Therefore, since $d\lambda_D$ is constant, our maximization problem becomes:

$$\max_{P_k^j} g(P_k^j) = \sum_{k=1}^{D-1} \sum_{j=1}^d (\lambda_k - \lambda_D) P_k^j \qquad s.t. \qquad \begin{cases} P_k^j \ge 0, \\ \sum_{k=1}^{D-1} P_k^j \le 1, \\ \sum_{j=1}^d P_k^j \le 1. \end{cases}$$
(A30)

This is now a linear program (LP) that can be recasted in the following matrix form:

$$\max_{\mathbf{x}} g = \mathbf{c}^T \mathbf{x} \qquad s.t. \quad \begin{cases} \mathbf{A} \mathbf{x} \le \mathbf{b}, \\ \mathbf{x} \ge 0, \end{cases}$$
 (A31)

where we have defined:

$$\mathbf{x} = \begin{bmatrix} P_1^1 \\ \vdots \\ P_1^d \\ P_2^1 \\ \vdots \\ P_2^d \\ \vdots \\ P_{D-1}^d \\ \vdots \\ P_{D-1}^d \end{bmatrix} d, \quad \mathbf{c} = \begin{bmatrix} \lambda_1 - \lambda_D \\ \vdots \\ \lambda_1 - \lambda_D \\ \lambda_2 - \lambda_D \\ \vdots \\ \lambda_2 - \lambda_D \\ \vdots \\ \lambda_{D-1} - \lambda_D \\ \vdots \\ \lambda_{D-1} - \lambda_D \end{bmatrix} d, \quad \mathbf{b} = \begin{bmatrix} 1 \\ 1 \\ \vdots \\ 1 \\ 1 \\ \vdots \\ 1 \end{bmatrix} d$$

$$(A32)$$

$$\mathbf{A} = \begin{bmatrix} d & d & d \\ 11 \dots 1 & 00 \dots 0 & \cdots & 00 \dots 0 \\ 00 \dots 0 & 11 \dots 1 & \cdots & 00 \dots 0 \\ \vdots & \vdots & & \vdots \\ 00 \dots 0 & 00 \dots 0 & \cdots & 11 \dots 1 \\ 10 \dots 0 & 10 \dots 0 & \cdots & 10 \dots 0 \\ 01 \dots 0 & 01 \dots 0 & \cdots & 01 \dots 0 \\ \vdots & \vdots & & \vdots \\ 00 \dots 1 & 00 \dots 1 & \cdots & 00 \dots 1 \end{bmatrix} \right\} d$$
(A33)

The recasting is useful, because it allows us to use the *strong duality theorem* [61, 62] to solve the problem². Indeed, we can derive the following *dual* LP:

$$\min_{\mathbf{y}} g^* = \mathbf{b}^T \mathbf{y} \qquad s.t. \quad \begin{cases} \mathbf{A}^T \mathbf{y} \ge \mathbf{c}, \\ \mathbf{y} \ge 0, \end{cases}$$
(A38)

where we have defined:

$$\mathbf{A}^{T} = \begin{bmatrix} D-1 & d \\ 1 & 0 & 0 \dots 0 & 1 & 0 \dots 0 \\ \vdots & \vdots & \vdots & \vdots & \vdots & \vdots \\ 1 & 0 & 0 \dots 0 & 0 & 0 \dots 1 \\ 0 & 1 & 0 \dots 0 & 1 & 0 \dots 0 \\ \vdots & \vdots & \vdots & \vdots & \vdots & \vdots \\ 0 & 1 & 0 \dots 0 & 0 & 0 \dots 1 \\ \vdots & \vdots & \vdots & \vdots & \vdots & \vdots \\ 0 & 0 & 0 \dots 1 & 1 & 0 \dots 0 \\ \vdots & \vdots & \vdots & \vdots & \vdots & \vdots \\ 0 & 0 & 0 \dots 1 & 0 & 0 \dots 1 \end{bmatrix} d , \quad \mathbf{y} = \begin{bmatrix} y_{1} \\ y_{2} \\ \vdots \\ y_{D-1} \\ y_{D} \\ \vdots \\ y_{D-1+d} \end{bmatrix} d . \quad (A39)$$

Therefore, explicitly the *dual* LP in (A38) becomes:

$$\min_{\mathbf{y}} g^* = \sum_{k=1}^{D-1+d} y_k \qquad s.t \qquad \begin{cases} y_1 + y_D \ge \lambda_1 - \lambda_D, \\ y_1 + y_{D+1} \ge \lambda_1 - \lambda_D, \\ \vdots \\ y_1 + y_{D-1+d} \ge \lambda_1 - \lambda_D, \end{cases} d \\
\vdots \\
y_{D-1} + y_D \ge \lambda_{D-1} - \lambda_D, \\
y_{D-1} + y_{D+1} \ge \lambda_{D-1} - \lambda_D, \\
\vdots \\
y_{D-1} + y_{D-1+d} \ge \lambda_{D-1} - \lambda_D, \end{cases} d$$

$$\vdots \\
y_{D-1} + y_{D-1+d} \ge \lambda_{D-1} - \lambda_D, \end{cases} d$$

In order to minimize the function g^* we can expand the summation:

$$g^* = \sum_{k=1}^{D-1+d} y_k = y_1 + y_2 + \dots + y_d + \dots + y_{D-1} + y_D + \dots + y_{D-1+d},$$
(A41)

$$g^* = \mathbf{b}^T \mathbf{y},\tag{A34}$$

and we try to find which coefficients minimize this linear combination in order to approximate the upper-bound of g. This defines the *dual* LP:

$$\min_{\mathbf{y}} g^* = \mathbf{b}^T \mathbf{y} \qquad s.t. \quad \begin{cases} \mathbf{A}^T \mathbf{y} \ge \mathbf{c}, \\ \mathbf{y} \ge 0. \end{cases}$$
 (A35)

According to the *weak duality theorem*, for each feasible solution \mathbf{x} of the *primal* and each feasible solution \mathbf{y} of the *dual*, we have that:

$$\max_{\mathbf{x}} g = \mathbf{c}^T \mathbf{x} \le \min_{\mathbf{y}} g^* = \mathbf{b}^T \mathbf{y}. \tag{A36}$$

Then, for the *strong duality theorem*, if one of the two problems has an optimal solution, the same is valid for the other too and we have:

$$\max_{\mathbf{x}} \mathbf{c}^T \mathbf{x} = \min_{\mathbf{y}} \mathbf{b}^T \mathbf{y}, \tag{A37}$$

and this holds if and only if the duality gap is 0.

² In general, given a *linear program* (LP) as the one presented in (A31) (called *primal*), it is possible to construct the so called *dual* LP. Intuitively, in order to maximize the expression in (A31) we create a linear combination of the constraints b with positive coefficients y:

and group the terms in the following way:

$$g^* = (y_1 + y_D) + (y_2 + y_{D+1}) + \dots + (y_d + y_{D-1+d}) + \sum_{k=d+1}^{D-1} y_k$$

$$\geq (\lambda_1 - \lambda_D) + (\lambda_2 - \lambda_D) + \dots + (\lambda_d - \lambda_D) + \sum_{k=d+1}^{D-1} y_k,$$
(A42)

where in the last inequality we have used the constraints in (A40).

Without loss of generality we can decompose the state ψ in (A3) such that its spectrum:

$$\lambda(\psi) = \{\lambda_k : \lambda_1 \ge \lambda_2 \ge \dots \ge \lambda_D\}. \tag{A43}$$

With such a decomposition we will have that:

$$\lambda_1 - \lambda_D \ge \lambda_2 - \lambda_D \ge \dots \ge \lambda_{D-1} - \lambda_D,\tag{A44}$$

and therefore we can minimize g^* by choosing $y_{d+1} = \cdots = y_{D-1} = 0$, since this will always satisfy the constraints in $(A40)^3$. In this way we can cancel the last term in (A42) and derive the following lower bound:

$$g^* \ge \sum_{i=1}^d \lambda_i - d\lambda_D. \tag{A47}$$

Now we can go back to the *primal* LP in (A31) and observe that there exists a specific choice of values for the variables $\{P_k^j\}$ such that:

$$g(P_k^j) = \sum_{i=1}^d \lambda_i - d\lambda_D, \qquad \text{for the choice:} \qquad \begin{cases} P_k^j = \frac{1}{d}, & \forall k = 1, ..., d, \\ P_k^j = 0, & otherwise. \end{cases}$$
(A48)

Therefore, there exists a feasible solution (A48) of the *primal* LP and a feasible solution (A47) of the *dual* LP for which the *primal* and the *dual* coincide. Since from the *strong duality theorem* (A37) we know that this is possible only in presence of an *optimal* solution for both problems, we can realize that the one found in (A48) is precisely the solution of the maximization problem in (A30).

Now, by inserting this solution into (A29), we can solve the original problem (A28):

$$\max_{P_k^j} \sqrt{\sum_{j=1}^d \sum_{k=1}^D \lambda_k P_k^j} = \sqrt{\sum_{i=1}^d \lambda_i}.$$
 (A49)

By remembering that the LHS of the latter is the result of the maximization over $\{\mu_j\}$ of (A20), we can finally maximize the fidelity in (A19) and find that:

$$F(\phi^S, \psi^S) \le \sum_{i=1}^d \lambda_i,\tag{A50}$$

that, combined with (A4) gives the Result 1.

$$y_{d+1} + y_D \ge \lambda_{d+1} - \lambda_D \implies y_D \ge \lambda_{d+1} - \lambda_D.$$
 (A45)

This imposes a lower bound on the value of y_D , that shouldn't be in contrast with all the other constraints. However, since the spectrum of the state

satisfies (A43), the following are still valid:

$$y_i + y_D \ge \lambda_i - \lambda_D \qquad \forall i = \{1, ..., d, ..., D - 1\}.$$
 (A46)

The same will happen with the values $y_{D+1}, \ldots, y_{D-1+d}$, once we impose the other constraints: also in those cases we will find lower bounds that are not in contrast with each other.

³ We can give an explicit example. Let's choose $y_{d+1}=0$. Then from the constraints of problem (A40) we will have:

Appendix B: Fidelity witness for GHZ, cluster and AME states

In this section we evaluate the bound on the fidelity (Result 1) for any state ρ with GME-dimension no larger than $d_{\rm GME}$, with three different seminal families of n-partite pure target states: GHZ states, AME states and linear cluster states. In all the cases we need to find the bipartition $(S|\bar{S})$ for which the sum of the first $d_{\rm GME}$ eigenvalues, ordered non-increasingly, of the reduced state is maximum.

• GHZ state

Since the n-partite GHZ state $|\mathrm{ghz}_{n,d}\rangle = \frac{1}{\sqrt{d}}\sum_{k=0}^{d-1}|k\rangle^{\otimes n}$ is already expressed in its Schmidt decomposition, for any bipartition $(S|\bar{S})$ the spectrum of the reductions has always the same non-zero values $\{\lambda_i=1/d,\ i=1,\ldots,d\}$. Therefore, the fidelity bound in this case becomes

$$F_{\mathsf{ghz}_{n,d}}(\rho) \le \max_{\{S|\bar{S}\}} \sum_{i=1}^{d_{\mathsf{GME}}} \lambda_i = \frac{d_{\mathsf{GME}}}{d}. \tag{B1}$$

AME states

Also in this case the fidelity bound can be found by looking at the definition of the state. A n-partite state $|\psi\rangle$ is called absolutely maximally entangled (AME) if for any bipartition $(S|\bar{S})$ its reduction is maximally mixed, i.e. if we choose S to be always the smallest subset of the bipartition, we have that the spectrum of the reductions is $\{\lambda_i^S=1/d^{|S|}, i=1,\ldots,d^{|S|}\}$ for any $(S|\bar{S})$. Therefore, the bipartitions that maximize the sum of the first $d_{\rm GME}$ eigenvalues of the reductions are the ones such that |S|=1. Then the fidelity bound reads:

$$F_{\text{AME}}(\rho) \le \max_{\{S|\bar{S}\}} \sum_{i=1}^{d_{\text{GME}}} \lambda_i^S = \frac{d_{\text{GME}}}{d}.$$
 (B2)

• Linear cluster state

In this case the derivation of the fidelity bound is less straightforward than before, since it is not possible to obtain the spectrum of all possible reductions simply by looking at the generic expression of the linear cluster state,

$$|C_{n,d}\rangle = \frac{1}{d^{n/2}} \bigotimes_{a=1}^{n} \left(\sum_{k=0}^{d-1} |k\rangle_{a} Z_{a+1}^{k} \right) = \frac{1}{d^{n/2}} \sum_{k_{1}=0}^{d-1} |k_{1}\rangle \otimes \sum_{k_{2}=0}^{d-1} Z^{k_{1}} |k_{2}\rangle \otimes \cdots \otimes \sum_{k_{n}=0}^{d-1} Z^{k_{n-1}} |k_{n}\rangle$$

$$= \frac{1}{d^{n/2}} \sum_{k_{1}, \dots, k_{n}=0}^{d-1} \omega^{k_{1}k_{2} + \dots + k_{n-1}k_{n}} |k_{1} \dots k_{n}\rangle.$$
(B3)

Therefore, we can proceed in a different way. Fix the number of parties n. Let us group all possible bipartitions $(S|\bar{S})$ whose smallest subset S has the same cardinality |S| in collections $\mathcal{B}_{|S|}^4$. We can realize that for all the bipartitions living in the same collection, the reductions can only have a finite number of possible structures.

As an example, let us fix n=6 and consider three possible bipartitions from the collection \mathcal{B}_3 : (123|456), (156|234) and (145|236). The reductions over the S subset are:

$$\operatorname{tr}_{123}(C_{6,d}) = \frac{1}{d^3} \sum_{k_4=0}^{d-1} \sum_{k_5, k_4'=0}^{d-1} \sum_{k_6, k_2'=0}^{d-1} \omega^{k_4(k_5-k_5')} \omega^{k_5k_6-k_5'k_6'} |k_4k_5k_6\rangle\langle k_4k_5'k_6'|,$$
(B4)

$$\operatorname{tr}_{156}(C_{6,d}) = \frac{1}{d^3} \sum_{k_2=0}^{d-1} \sum_{k_3, k_5'=0}^{d-1} \sum_{k_4=0}^{d-1} \omega^{(k_2+k_4)(k_3-k_3')} |k_2 k_3 k_4\rangle \langle k_2 k_3' k_4|,$$
(B5)

⁴ e.g. for n=4 we have two collections of bipartitions:

⁻ $\mathcal{B}_1 = \{(1|234), (2|134), (3|124), (4|123)\};$

⁻ $\mathcal{B}_2 = \{(12|34), (13|24), (14|23)\}.$

$$\operatorname{tr}_{145}(C_{6,d}) = \frac{1}{d^3} \sum_{k_2, k_3, k_6 = 0}^{d-1} |k_2 k_3 k_6\rangle \langle k_2 k_3 k_6|.$$
(B6)

These reductions have three different structures that can be distinguished by the number of k' terms in the tensor product of the basis vectors. By computing the other possible reductions in the collection \mathcal{B}_3 , we can realize that all the structures fall into one of these three cases. Indeed, in general, fixed the number of parties in our reduction, the whole set of possible matrices can be constructed by changing the position and the number of the k' terms.

Therefore, given a generic collection $\mathcal{B}_{|S|}$, where we label the elements in every subset S as $\{S_1, \ldots, S_p\}$, the reductions over the subsets \bar{S} can only have the following shapes:

$$\operatorname{tr}_{\bar{S}}(C_{n,d}) = \frac{1}{d^{|S|}} \begin{cases} \sum_{S_{1},\dots,S_{p}=0}^{d-1} |S_{1}\dots S_{p}\rangle\langle S_{1}\dots S_{p}|, \\ \sum_{S_{1}\leq S_{1}} \sum_{S_{i},S'_{i}=0}^{d-1} \omega^{(S_{i-1}+S_{i+1})(S_{i}-S'_{i})} |S_{1}\dots S_{i}\dots S_{p}\rangle\langle S_{1}\dots S'_{i}\dots S_{p}|, \\ \vdots \\ \sum_{S_{1}=0}^{d-1} \sum_{S_{2},S'_{2}=0}^{d-1} \cdots \sum_{S_{p},S'_{p}=0}^{d-1} \omega^{S_{1}(S_{2}-S'_{2})} \cdots \omega^{S_{p-1}S_{p}-S'_{p-1}S'_{p}} |S_{1}S_{2}\dots S_{p}\rangle\langle S_{1}S'_{2}\dots S'_{p}|. \end{cases}$$
(B7)

To study the spectrum of all the reductions in the collection $\mathcal{B}_{|S|}$, then we need to diagonalize each of the possible matrices. By defining with $A'_m = \{S'_{i_1}, \dots, S'_{i_m}\}$ the generic set of the S' terms and with $A_m = \{S_{i_1}, \dots, S_{i_m}\}$ the set of the corresponding elements in the original subset, we can group all the cases in (B7) into a single expression:

$$\rho_S^m = \frac{1}{d^{|S|}} \sum_{S} \sum_{S'_{i_1}, \dots, S'_{i_m} = 0}^{d-1} \omega^{(S_{i_1-1} + S_{i_1+1})(S_{i_1} - S'_{i_1})} \dots \omega^{(S_{i_m-1} + S_{i_m+1})(S_{i_m} - S'_{i_m})} |S\rangle\langle (S \setminus A) \cup A'|,$$
(B8)

where $0 \le m \le |S| - 1$. Then it is possible to show that the following states

$$\left| g_{q_1 q_2 \dots q_{|S|}} \right\rangle = \frac{1}{\sqrt{d^{|S|}}} \sum_{l_1, \dots, l_{|S|} = 0}^{d-1} \omega^{l_1 l_2 + \dots + l_{|S|-1} l_{|S|}} \omega^{q_1 l_1 + \dots + q_{|S|-2} l_{|S|-2}} \left| l_1 \dots l_{|S|-2} \left(l_{|S|-1} - q_{|S|-1} \right) \left(l_{|S|} - q_{|S|} \right) \right\rangle$$
(B9)

with $q_1, q_2, \dots, q_{|S|} \in \{0, \dots, d-1\}$ diagonalize the matrix (B8) such that

$$\rho_S^m \left| g_{q_1 q_2 \dots q_{|S|}} \right\rangle = \frac{1}{d^{|S|-m}} \left| g_{q_1 q_2 \dots q_{|S|}} \right\rangle. \tag{B10}$$

With this result we can now calculate the fidelity bound. Indeed, we have shown that for any bipartition $(S|\bar{S})$ the spectrum of the reduction is always uniform with values within $\{1/d,\ldots,1/d^{|S|}\}$. Therefore, the sum of the first d_{GME} eigenvalues is maximum for the bipartitions $(S|\bar{S})$ in which $\{\lambda_i^S=1/d,\quad i=1,\ldots,d\}$ and the fidelity bound reads:

$$F_{\text{cluster}}(\rho) \le \max_{\{S|\bar{S}\}} \sum_{i=1}^{d_{\text{GME}}} \lambda_i = \frac{d_{\text{GME}}}{d}.$$
(B11)

 $\left|S\right|-1.$ However, this detail is not so relevant for the derivation of the fidelity bound.

⁵ Because of the shape of the linear cluster state in (B3), for a reduction of |S| parties it is not possible to have a number of S' terms larger than

Appendix C: Proof of Result 2

Let us consider the following operator:

$$O_{n,d}^{\text{ghz}} = \sum_{j=0}^{d-1} |j\rangle\langle j|^{\otimes n} + \sum_{j_1,\dots,j_n=0}^{d-1} \bigotimes_{l=1}^{n} |e_{j_l}\rangle\langle e_{j_l}| \,\delta_{j_1 \oplus \dots \oplus j_n,0},\tag{C1}$$

where \oplus denotes addition modulo d, $\{|j\rangle\}_{j=0}^{d-1}$ is the computational basis and $\{|e_j\rangle\}_{j=0}^{d-1}$ is the Fourier basis obtained from

$$|e_j\rangle = \frac{1}{\sqrt{d}} \sum_{k=0}^{d-1} \omega^{jk} |k\rangle, \quad \text{with: } \omega = e^{\frac{2\pi i}{d}}.$$
 (C2)

The proof of our result for the entanglement witness $\mathcal{W}_{n,d}^{\text{ghz}}(\rho) = \operatorname{tr}\left(\rho O_{n,d}^{\text{ghz}}\right)$ can be provided in three steps:

• Show that $|ghz_{n,d}\rangle$ has perfect correlations for $O_{n,d}^{ghz}$ and therefore $\mathcal{W}_{n,d}^{ghz}(|ghz_{n,d}\rangle)=2$.

For simplicity, let us separately consider the measurement operators in $O_{n,d}^{\mathrm{ghz}}$:

$$A = \sum_{j=0}^{d-1} |j\rangle\langle j|^{\otimes n}, \qquad B = \sum_{j_1,\dots,j_n=0}^{d-1} \bigotimes_{l=1}^n |e_{j_l}\rangle\langle e_{j_l}| \,\delta_{j_1\oplus\dots\oplus j_n,0}. \tag{C3}$$

and show that $|ghz_{n,d}\rangle$ is an eigenstate of both A and B.

For A we can use the orthonormality of the computational basis $\langle l|x\rangle=\delta_{lx}$ to get that $|\mathrm{ghz}_{n,d}\rangle$ is an eigenstate. For B the situation is slightly different:

$$B\left|\operatorname{ghz}_{n,d}\right\rangle = \left(\sum_{j_1,\dots,j_n=0}^{d-1} \bigotimes_{l=1}^{n} |e_{j_l}\rangle\langle e_{j_l}| \,\delta_{j_1\oplus\dots\oplus j_n,0}\right) \frac{1}{\sqrt{d}} \sum_{x=0}^{d-1} |x\rangle^{\otimes n} \,. \tag{C4}$$

By using the definition (C2) of the Fourier basis, we get:

$$B\left|\operatorname{ghz}_{n,d}\right\rangle = \frac{1}{\sqrt{d}} \sum_{j_1 \oplus \dots \oplus j_n = 0} \sum_{x=0}^{d-1} \left(\frac{1}{\sqrt{d^n}} \sum_{k_1, \dots, k_n = 0}^{d-1} \omega^{-k_1 j_1} \dots \omega^{-k_n j_n} \underbrace{\langle k_1 \dots k_n | x \dots x \rangle}_{\delta_{k_i x}} \right) \left| e_{j_1} \dots e_{j_n} \right\rangle$$

$$= \frac{1}{\sqrt{d^{n+1}}} \sum_{j_1 \oplus \dots \oplus j_n = 0} \sum_{x=0}^{d-1} \omega^{-\sum_{\gamma=1}^n j_{\gamma} x} \left| e_{j_1} \dots e_{j_n} \right\rangle = \frac{1}{\sqrt{d^{n-1}}} \sum_{j_1 \oplus \dots \oplus j_n = 0} \left| e_{j_1} \dots e_{j_n} \right\rangle.$$
(C5)

By performing a change of basis, we can show that this state is actually the original GHZ state. Indeed, if we consider that

$$|x\rangle = \sum_{j=0}^{d-1} |e_j\rangle \langle e_j|x\rangle = \sum_{j=0}^{d-1} |e_j\rangle \frac{1}{\sqrt{d}} \sum_{k=0}^{d-1} \omega^{-kj} \underbrace{\langle k|x\rangle}_{\delta} = \frac{1}{\sqrt{d}} \sum_{j=0}^{d-1} \omega^{-jx} |e_j\rangle, \tag{C6}$$

we can rewrite

$$\left| \mathsf{ghz}_{n,d} \right\rangle = \frac{1}{\sqrt{d}} \sum_{x=0}^{d-1} |x\rangle^{\otimes n} = \frac{1}{\sqrt{d}} \frac{1}{\sqrt{d^n}} \sum_{j_1, \dots, j_n = 0}^{d-1} \left(\sum_{x=0}^{d-1} \omega^{-\sum_{\gamma} j_{\gamma} x} \right) |e_{j_1} \dots e_{j_n}\rangle = \frac{1}{\sqrt{d^{n-1}}} \sum_{j_1 \oplus \dots \oplus j_n = 0} |e_{j_1} \dots e_{j_n}\rangle, \quad (C7)$$

where in the last equality we have used that the sum over x is a geometric series:

$$\sum_{x=0}^{d-1} \omega^{-Jx} = \frac{1 - \omega^{-Jd}}{1 - \omega^{-J}} = \begin{cases} 0 & \leftrightarrow J \neq 0, \\ d & \leftrightarrow J = 0 \pmod{d}, \end{cases}$$
 (C8)

with $J := \sum_{\gamma=1}^{n} j_{\gamma}$. We can realize that the final state in (C7) is precisely the one obtained in (C5) and therefore we can conclude that:

$$\begin{cases} A \left| \mathsf{ghz}_{n,d} \right\rangle = \left| \mathsf{ghz}_{n,d} \right\rangle, \\ B \left| \mathsf{ghz}_{n,d} \right\rangle = \left| \mathsf{ghz}_{n,d} \right\rangle \end{cases} \implies O_{n,d}^{\mathsf{ghz}} \left| \mathsf{ghz}_{n,d} \right\rangle = 2 \left| \mathsf{ghz}_{n,d} \right\rangle. \tag{C9}$$

• Show that the spectral decomposition of $O_{n,d}^{ghz}$ is $\lambda(O_{n,d}^{ghz}) = \{\lambda_{ghz_{n,d}}, \lambda_2, \dots, \lambda_{d^n}\}$ such that $\lambda_i \leq 1 \quad \forall i \neq ghz_{n,d}$ Since $O_{n,d}^{ghz} \geq 0$, it admits a spectral decomposition:

$$O_{n,d}^{\text{ghz}} = \sum_{i=1}^{d^n} \lambda_i |\lambda_i\rangle \langle \lambda_i|. \tag{C10}$$

From the previous step we know that one of the possible eigenstates is the $|\text{ghz}_{n,d}\rangle$ state for which $\lambda_{\text{ghz}_{n,d}}=2$. Therefore, we can write that

$$O_{n,d}^{\text{ghz}} = 2 \left| \text{ghz}_{n,d} \middle\rangle \left(\text{ghz}_{n,d} \right) + \sum_{i=2}^{d^n} \lambda_i \left| \lambda_i \middle\rangle \left\langle \lambda_i \right|.$$
 (C11)

For simplicity, let us define $\mathrm{ghz}_{n,d} = \left| \mathrm{ghz}_{n,d} \right\rangle \left\langle \mathrm{ghz}_{n,d} \right|$ and let us decompose the previous expression as

$$O_{n,d}^{\text{ghz}} = \text{ghz}_{n,d} + \left(\text{ghz}_{n,d} + \sum_{i=2}^{d^n} \lambda_i |\lambda_i\rangle\langle\lambda_i|\right),\tag{C12}$$

so that we can define the following shifted operator:

$$\tilde{O}_{n,d}^{\rm ghz} = O_{n,d}^{\rm ghz} - {\rm ghz}_{n,d}. \tag{C13}$$

We now prove that this shifted operator is a projector, and consequently that all its eigenvalues are either zero or one. To do that we calculate its square:

$$(\tilde{O}_{n,d}^{\rm ghz})^2 = (O_{n,d}^{\rm ghz})^2 + {\rm ghz}_{n,d} - \{O_{n,d}^{\rm ghz}, {\rm ghz}_{n,d}\}, \tag{C14}$$

where the anticommutator can be computed by using (C9):

$$\left\{O_{n,d}^{\mathrm{ghz}},\mathrm{ghz}_{n,d}\right\} = O_{n,d}^{\mathrm{ghz}}\left|\mathrm{ghz}_{n,d}\right\rangle\!\!\left\langle\mathrm{ghz}_{n,d}\right| + \left|\mathrm{ghz}_{n,d}\right\rangle\!\!\left\langle\mathrm{ghz}_{n,d}\right| O_{n,d}^{\mathrm{ghz}} = 4\,\mathrm{ghz}_{n,d}. \tag{C15}$$

The $(O_{n,d}^{\rm ghz})^2$ term instead can be calculated by using the definition (C1):

$$(O_{n,d}^{\text{ghz}})^{2} = \left[\sum_{j=0}^{d-1} |j\rangle\langle j|^{\otimes n} + \sum_{j_{1},\dots,j_{n}=0}^{d-1} \bigotimes_{l=1}^{n} |e_{j_{l}}\rangle\langle e_{j_{l}}| \,\delta_{j_{1}\oplus\dots\oplus j_{n},0} \right] \cdot \left[\sum_{j'=0}^{d-1} |j'\rangle\langle j'|^{\otimes n} + \sum_{j'_{1},\dots,j'_{n}=0}^{d-1} \bigotimes_{l=1}^{n} \left| e_{j'_{l}} \right\rangle\langle e_{j'_{l}} \left| \,\delta_{j'_{1}\oplus\dots\oplus j'_{n},0} \right| ,$$
(C16)

in which we can simplify the non-mixing terms by using the orthonormality of both computational and Fourier basis:

$$(O_{n,d}^{\text{ghz}})^{2} = \underbrace{\sum_{j=0}^{d-1} |j\rangle\langle j|^{\otimes n}}_{j_{1},\dots,j_{n}=0} + \underbrace{\sum_{j=1}^{d-1} \bigotimes_{j_{1},\dots,j_{n}=0}^{n} |e_{j_{l}}\rangle\langle e_{j_{l}}| \delta_{j_{1}\oplus\dots\oplus j_{n},0}}_{O_{n,d}^{\text{ghz}}}$$

$$+ \underbrace{\sum_{j=0}^{d-1} |j\dots j\rangle \underbrace{\langle j\dots j| e_{j'_{1}}\dots e_{j'_{n}}\rangle}_{\frac{1}{\sqrt{d^{n}}}\omega^{J'j}} \langle e_{j'_{1}}\dots e_{j'_{n}}| + \underbrace{\sum_{j'=0}^{d-1} |j'\dots j'\rangle}_{j_{1}\oplus\dots\oplus j_{n}=0} |j'\dots j'\rangle \underbrace{\langle j'\dots j'| e_{j_{1}}\dots e_{j_{n}}\rangle}_{\frac{1}{\sqrt{d^{n}}}\omega^{-Jj'}} \langle e_{j_{1}}\dots e_{j_{n}}|,$$

$$(C17)$$

where we are using $J\coloneqq\sum_{\gamma=1}^n j_\gamma$ and $J'\coloneqq\sum_{\gamma=1}^n j'_\gamma.$ We end up with

$$(O_{n,d}^{\text{ghz}})^{2} = O_{n,d}^{\text{ghz}} + \sum_{\substack{j=0\\j'_{1} \oplus \cdots \oplus j'_{n} = 0}}^{d-1} \frac{1}{\sqrt{d}} |j \dots j\rangle \left\langle e_{j'_{1}} \dots e_{j'_{n}} \right| \frac{1}{\sqrt{d^{n-1}}} + \sum_{\substack{j'=0\\j_{1} \oplus \cdots \oplus j_{n} = 0}}^{d-1} \frac{1}{\sqrt{d^{n-1}}} |e_{j_{1}} \dots e_{j_{n}}\rangle \left\langle j' \dots j' \right| \frac{1}{\sqrt{d}}. \quad (C18)$$

By looking at (C7) we can realize that the previous expression can be simply written as

$$(O_{n,d}^{\text{ghz}})^2 = O_{n,d}^{\text{ghz}} + 2\,\text{ghz}_{n,d}. \tag{C19}$$

Now we can insert this result into (C14) and get

$$(\tilde{O}_{n,d}^{\rm ghz})^2 = (O_{n,d}^{\rm ghz})^2 + {\rm ghz}_{n,d} - 4\,{\rm ghz}_{n,d} = O_{n,d}^{\rm ghz} - {\rm ghz}_{n,d} = \tilde{O}_{n,d}^{\rm ghz}, \tag{C20}$$

which proves that $\tilde{O}_{n,d}^{\rm ghz}$ is a projector.

• Derivation of the upper bound for $W_{n,d}^{ghz}(\rho) = \operatorname{tr}\left(\rho O_{n,d}^{ghz}\right)$

In order to maximize the witness, we can now use the spectral decomposition (C12) of the operator $O_{n,d}^{\text{ghz}}$.

$$\mathcal{W}_{n,d}^{\text{ghz}}(\rho) = \operatorname{tr}\left(\rho O_{n,d}^{\text{ghz}}\right) = F_{\text{ghz}_{n,d}}(\rho) + \operatorname{tr}\left(\rho\left(\text{ghz}_{n,d} + \sum_{i=2}^{d^n} \lambda_i |\lambda_i\rangle\langle\lambda_i|\right)\right) \le F_{\text{ghz}_{n,d}}(\rho) + 1, \tag{C21}$$

where in the last inequality we have used that

$$\lambda(O_{n,d}^{\mathsf{ghz}}) = \{2, \lambda_2, \dots, \lambda_{d^n} : \lambda_i \le 1\} \quad \Longrightarrow \quad \mathsf{ghz}_{n,d} + \sum_{i=2}^{d^n} \lambda_i \, |\lambda_i\rangle\!\langle\lambda_i| \le \mathbb{1}. \tag{C22}$$

We can realize that $F_{\text{ghz}_{n,d}}(\rho)$ is the fidelity between a n-partite pure GHZ state and a state ρ with $\mathcal{D}_{\textit{GME}}(\rho) \leq d_{\textit{GME}}$, that can be bounded using Result 1 as shown in (B1). By inserting this result into (C21) we get:

$$W_{n,d}^{\text{ghz}}(\rho) \le 1 + \frac{d_{\text{GME}}}{d},$$
 (C23)

that is the result we wanted to prove. Moreover, by looking at the last inequality in (C21) we can realize that

$$F_{\operatorname{ghz}_{n,d}}(\rho) \ge \mathcal{W}_{n,d}^{\operatorname{ghz}}(\rho) - 1. \tag{C24}$$

Appendix D: Optimality of minimal witness for dephased GHZ state

The proof of this result parallels the approach used in [24] to prove the tightness of the fidelity bound in the case of a dephased bipartite maximally entangled state. We consider a dephased high-dimensional n-partite GHZ state,

$$\rho = v \left| \mathsf{ghz}_{n,d} \middle\backslash \mathsf{ghz}_{n,d} \right| + \frac{1 - v}{d} \sum_{i=0}^{d-1} |i \middle\backslash i|^{\otimes n} = \frac{1}{d} \sum_{i=0}^{d-1} |i \middle\backslash i|^{\otimes n} + \frac{v}{d} \sum_{i \neq j=0}^{d-1} |i \middle\backslash j|^{\otimes n} \,, \tag{D1}$$

where in the second equality we wrote the state by expanding GHZ in the computational basis for later convenience. From Result 1 we know that, if the GME-dimension of ρ is no larger than $d_{\rm GME}$, then its fidelity with the GHZ state is bounded by

$$F_{\text{ghz}}(\rho) \le \max_{\{S|\bar{S}\}} \sum_{i=1}^{d_{\text{GME}}} \lambda_i = \frac{d_{\text{GME}}}{d},\tag{D2}$$

where we used that the spectrum of the reductions of $\operatorname{ghz}_{n,d}$ over all possible bipartitions is always $\{\lambda_i=1/d,\quad i=1,\dots,d\}$. Now we can prove that a dephased GHZ state fulfilling this bound necessarily has a GME-dimension no larger than d_{GME} . We can start by considering that for any d_{GME} it is always possible to find a critical visibility v^* and the associated state ρ^* such that $F_{\operatorname{ghz}}(\rho^*)=d_{\operatorname{GME}}/d$, since

$$F_{\text{ghz}}(\rho^*) = v^* + \frac{1 - v^*}{d} = \frac{d_{\text{GME}}}{d} \implies v^* = \frac{d_{\text{GME}} - 1}{d - 1}.$$
 (D3)

Then, to prove our result, we only need to show that this state ρ^* has a GME-dimension no larger than d_{GME} . We can consider the family of all pure states with GME-dimension equal to d_{GME} :

$$|\Phi_{\alpha}\rangle = \frac{1}{\sqrt{|\alpha|}} \sum_{i \in \alpha} |i\rangle^{\otimes n},$$
 (D4)

where $\alpha \subset \{0, 1, \dots, d-1\}$ with cardinality $|\alpha| = d_{\text{GME}}$. They are in total $\binom{d}{d_{\text{GME}}}$, so that we can take their incoherent mixture

$$\rho_{d_{\text{GME}}} = \frac{1}{\binom{d}{d_{\text{GME}}}} \sum_{\alpha \text{ s.t. } |\alpha| = d_{\text{GME}}} |\Phi_{\alpha}\rangle\langle\Phi_{\alpha}| = \frac{1}{\binom{d}{d_{\text{GME}}}} \sum_{\alpha \text{ s.t. } |\alpha| = d_{\text{GME}}} \frac{1}{|\alpha|} \left[\sum_{i \in \alpha} |i\rangle\langle i|^{\otimes n} + \sum_{i \neq j \in \alpha} |i\rangle\langle j|^{\otimes n} \right]. \tag{D5}$$

We can realize that each diagonal term on the RHS will appear in $\binom{d-1}{d_{\text{GME}}-1}$ possible α subsets while each off-diagonal term will appear in $\binom{d-2}{d_{\text{GME}}-2}$ possible α subsets. Therefore, we will have:

$$\rho_{d_{\text{GME}}} = \frac{1}{\binom{d}{d_{\text{GME}}}} \frac{1}{|\alpha|} \left[\binom{d-1}{d_{\text{GME}-1}} \sum_{i=0}^{d-1} |i\rangle\langle i|^{\otimes n} + \binom{d-2}{d_{\text{GME}}-2} \sum_{i\neq j=0}^{d-1} |i\rangle\langle j|^{\otimes n} \right] \\
= \frac{1}{d} \sum_{i=0}^{d-1} |i\rangle\langle i|^{\otimes n} + \left(\frac{d_{\text{GME}}-1}{d-1} \right) \frac{1}{d} \sum_{i\neq j=0}^{d-1} |i\rangle\langle j|^{\otimes n} \tag{D6}$$

that, considering the expression shown in (D1) of a generic dephased GHZ state, turns out to be precisely the state ρ^* . We can now remember that this state was constructed by taking a convex combination of pure states with GME-dimension equal to $d_{\rm GME}$ and therefore cannot have GME-dimension larger that $d_{\rm GME}$. Then we conclude that any dephased GHZ state ρ^* whose $F_{\rm ghz}(\rho^*) \leq d_{\rm GME}/d$ has GME-dimension no larger than $d_{\rm GME}$.

Appendix E: Three-partite witness for odd-dimensional GHZ states

Define the computational basis $\{|l\rangle\}_{l=0}^{d-1}$ and another d bases as $\left|e_l^{(j)}\right\rangle = \frac{1}{\sqrt{d}}\sum_{m=0}^{d-1}\omega^{m(l+jm)}\left|m\right\rangle$ with basis index $j=0,\ldots,d-1$ and element index $l=0,\ldots,d-1$. In odd prime dimensions, this happens to consitute a complete set of mutually unbiased bases. We consider a three-partite state in any odd local dimension d. We will use a total of ten global product measurements to witness the GME-dimension via fidelity estimation. The first global product measurement corresponds to the computational basis. The other nine correspond to the following tuples indexing the basis index j for each of the three parties;

$$L = \{(0,0,0), (1,1,d-2), (d-1,d-1,2), (0,1,d-1), (1,0,d-1), (0,d-1,1), (1,d-1,0), (d-1,0,1), (d-1,1,0)\}. \ \ (\text{E1}) = \{(0,0,0), (1,1,d-2), (d-1,d-1,2), (0,1,d-1), (1,0,d-1), (0,d-1,1), (1,d-1,0), (1,d-1,0),$$

Based on these measurements, we define the entanglement witness operator

$$W_d = 3\sum_{l=0}^{d-1} |l\rangle\langle l|^{\otimes 3} + \sum_{(j_1, j_2, j_3) \in L} \sum_{l_1 \oplus l_2 \oplus l_3 = 0}^{d-1} \bigotimes_{k=1}^{3} \left| e_{l_k}^{(j_k)} \right\rangle \langle e_{l_k}^{(j_k)} \right|.$$
 (E2)

The corresponding entanglement witness quantity is therefore $W_d = \operatorname{tr}(W_d \rho)$. In the case of a GHZ state, one has perfect correlations in each of the ten measurements and hence obtains $W_d = 12$. For an arbitrary three-partite state ρ of equal odd local dimension d, it holds that

$$W_d \le 3 + \frac{9\mathcal{D}_{\text{GME}}(\rho)}{d}.\tag{E3}$$

Moreover, any observed witness value implies a GHZ-fidelity bound of

$$F_{\text{ghz}}(\rho) \ge \frac{W_d - 3}{9}.\tag{E4}$$

We have shown this explicitly for odd $d \le 17$ and conjecture it to hold for odd d in general. The proof is based on explicitly computing the spectrum of W_d . All eigenvalues are non-negative by construction. Moreover, one eigenvector is the GHZ state with eigenvalue 12. For $d = 3, 5, \ldots, 17$ we observe that all other eigenvalues are no larger than 3. Hence, we can write

$$\mathcal{W}_d \leq 9 \left| \mathsf{ghz}_{n,d} \middle\rangle \mathsf{ghz}_{n,d} \right| + 31.$$
 (E5)

Taking the expectation value of both sides w.r.t. the state ρ and using that $F_{\rm ghz}(\rho) \leq \frac{d_{\rm GME}}{d}$ gives Eq. (E3).

When applied to the noisy GHZ state $\rho_v^{\rm ghz} = v \left| {\rm ghz}_{n,d} \right\rangle \left\langle {\rm ghz}_{n,d} \right| + \frac{1-v}{d^3} \mathbb{1}$, the critical visibility for detecting the GME-dimension is

$$v_{\text{crit}}^{10 \text{ bases}} = \frac{d^2 - 1 + 3d(d_{\text{GME}} - 1)}{4d^2 - 3d - 1}.$$
 (E6)

This can be compared to

$$v_{\text{crit}}^{\text{exact}} = \frac{d_{\text{GME}}d^2 - 1}{d^3 - 1},\tag{E7}$$

for exact fidelity measurements on a three-partite state. Note that for d=3, both formulas are identical. For d>3 the trade-off in resource-efficiency and detection power can be quantified via the impact parameter $\Delta=\frac{1-v_{\rm crit}^{10\,{\rm base}}}{1-v_{\rm crit}^{\rm exact}}$. For the most interesting case when $d_{\rm GME}=d-1$, this becomes

$$\Delta = \frac{3(1+d+d^2)}{d(1+4d)}.$$
(E8)

As expected, this is monotonically decreasing, since for larger d the number of extra measurements needed for the exact fidelity grows. However, even in the limit of $d \to \infty$ we have $\Delta = \frac{3}{4}$, showing that even for very large d, using just ten bases is still a decent bound on the true fidelity.

Appendix F: Proof of Result 3

Let us consider the following operator:

$$O_{n,d}^{\text{cluster}} = \bigotimes_{l \text{ odd } q_{l}, p_{l+1} = 0}^{n} \sum_{l \text{ odd } q_{l}, p_{l+1} = 0}^{d-1} |e_{q_{l}} p_{l+1}| \langle e_{q_{l}} p_{l+1} | \delta_{p_{l+1} \oplus p_{l-1} \ominus q_{l}, 0} + \bigotimes_{l \text{ odd } p_{l}, q_{l+1} = 0}^{n} \sum_{l \text{ odd } p_{l}, q_{l+1} = 0}^{d-1} |p_{l} e_{q_{l+1}}| \langle p_{l} e_{q_{l+1}} | \delta_{p_{l} \oplus p_{l+2} \ominus q_{l+1}, 0},$$
 (F1)

where \oplus denotes addition modulo d, $\{|j\rangle\}_{j=0}^{d-1}$ is the computational basis and $\{|e_j\rangle\}_{j=0}^{d-1}$ is the Fourier basis defined in (C2). By recalling the definition of the cluster state $|C_{n,d}\rangle$ given in (B3), we prove Result 3 in three steps as we did for Result 2 in Appendix C:

• Show that $|C_{n,d}\rangle$ has perfect correlations for $O_{n,d}^{cluster}$ and therefore $\mathcal{W}_{n,d}^{cluster}(|C_{n,d}\rangle)=2$.

In principle we can use the same procedure presented in the first step of Appendix C, i.e. to directly show that $|C_{n,d}\rangle$ is an eigenstate of the operator $O_{n,d}^{\text{cluster}}$. However, we here take the other, more informative, route, where we calculate the probability distribution for the two sets of global product bases used to construct the witness (F1). To do that, we separately consider the case where n is an even number and the case where n is odd.

- n-even

We can start by calculating the probability distribution for the measurements in the first term of (F1). In this case the n/2 subsystems $\{2, 4, \ldots, n\}$ are measured in the computational basis and the remaining n/2 subsystems $\{1, 3, \ldots, n-1\}$ are measured in the Fourier basis. Therefore, we get:

$$P(e_{q_{1}}, p_{2}, e_{q_{3}}, \dots, p_{n} | C_{n,d}) = |\langle e_{q_{1}} p_{2} e_{q_{3}} \dots p_{n} | C_{n,d} \rangle|^{2}$$

$$= \frac{1}{d^{n}} \left| \sum_{k_{1}, \dots, k_{n} = 0}^{d-1} \omega^{k_{1} k_{2} + \dots + k_{n-1} k_{n}} \frac{1}{\sqrt{d^{n/2}}} \sum_{l_{1}, l_{3}, \dots, l_{n-1} = 0}^{d-1} \omega^{-(l_{1} q_{1} + l_{3} q_{3} + \dots + l_{n-1} q_{n-1})} \langle l_{1} p_{2} l_{3} \dots p_{n} | k_{1} k_{2} k_{3} \dots k_{n} \rangle \right|^{2}$$

$$= \frac{1}{d^{n}} \frac{1}{d^{n/2}} \left| \sum_{k_{1}, k_{3}, \dots, k_{n-1} = 0}^{d-1} \omega^{k_{1} p_{2} + p_{2} k_{3} + k_{3} p_{4} + \dots + k_{n-1} p_{n}} \omega^{-(k_{1} q_{1} + k_{3} q_{3} + \dots + k_{n-1} q_{n-1})} \right|^{2}$$

$$= \frac{1}{d^{n}} \frac{1}{d^{n/2}} \left| \sum_{k_{1} = 0}^{d-1} \omega^{k_{1} (p_{2} - q_{1})} \sum_{k_{3} = 0}^{d-1} \omega^{k_{3} (p_{2} + p_{4} - q_{3})} \dots \sum_{k_{n-1} = 0}^{d-1} \omega^{k_{n-1} (p_{n-2} + p_{n} - q_{n-1})} \right|^{2},$$
(F2)

where in the last equality we can evaluate each of the sums with (C8) to end up with

$$P(e_{q_1}, p_2, e_{q_3}, \dots, p_n | C_{n,d}) = \frac{1}{d^{n/2}} \, \delta_{p_2 \oplus q_1, 0} \, \delta_{p_2 \oplus p_4 \oplus q_3, 0} \dots \delta_{p_{n-2} \oplus p_n \oplus q_{n-1}, 0}. \tag{F3}$$

Note that this probability distribution is uniform of $d^{n/2}$ possible outcomes and zero over the remaining $d^{n/2}$ outcomes. The former events coincide exactly with those used in the first term of the witness (F1). Hence,

$$\left(\bigotimes_{l \text{ odd}} \sum_{q_{l}, p_{l+1} = 0}^{d-1} |e_{q_{l}} p_{l+1}| \langle e_{q_{l}} p_{l+1} | \delta_{p_{l+1} \oplus p_{l-1} \ominus q_{l}, 0} \right) |C_{n,d}\rangle = |C_{n,d}\rangle.$$
 (F4)

The same approach applies to the second term in (F1). In this case we consider the n/2 subsystems $\{2, 4, ..., n\}$ to be measured in the Fourier basis and the remaining n/2 subsystems $\{1, 3, ..., n-1\}$ to be measured in the computational basis; then the probability distribution is

$$P(p_{1}, e_{q_{2}}, p_{3} \dots, e_{q_{n}} | C_{n,d}) = |\langle p_{1}e_{q_{2}}p_{3} \dots e_{q_{n}} | C_{n,d}\rangle|^{2}$$

$$= \frac{1}{d^{n}} \left| \sum_{k_{1}, \dots, k_{n} = 0}^{d-1} \omega^{k_{1}k_{2} + \dots + k_{n-1}k_{n}} \frac{1}{\sqrt{d^{n/2}}} \sum_{l_{2}, l_{4}, \dots, l_{n} = 0}^{d-1} \omega^{-(l_{2}q_{2} + l_{4}q_{4} + \dots + l_{n}q_{n})} \langle p_{1}l_{2}p_{3} \dots l_{n} | k_{1}k_{2}k_{3} \dots k_{n} \rangle \right|^{2}$$

$$= \frac{1}{d^{n/2}} \delta_{p_{1} \oplus p_{3} \oplus q_{2}, 0} \delta_{p_{3} \oplus p_{5} \oplus q_{4}, 0} \dots \delta_{p_{n-1} \oplus q_{n}, 0}.$$
(F5)

We observe an analogous structure, which corresponds to the second term in (F1), thus implying

$$\left(\bigotimes_{l \text{ odd}} \sum_{p_{l}, q_{l+1}=0}^{d-1} \left| p_{l} e_{q_{l+1}} \right| \left\langle p_{l} e_{q_{l+1}} \right| \delta_{p_{l} \oplus p_{l+2} \oplus q_{l+1}, 0} \right) \left| C_{n,d} \right\rangle = \left| C_{n,d} \right\rangle. \tag{F6}$$

n-odd

For the first term in (F1) we calculate the probability distribution for the $\frac{n+1}{2}$ subsystems $\{1,3,\ldots,n\}$ measured in the Fourier basis and the remaining $\frac{n-1}{2}$ subsystems $\{2,4,\ldots,n-1\}$ measured in the computational basis. We get:

$$P(e_{q_{1}}, p_{2}, e_{q_{3}}, \dots, p_{n-1}, e_{q_{n}} | C_{n,d}) = \left| \left\langle e_{q_{1}} p_{2} e_{q_{3}} \dots p_{n-1} e_{q_{n}} | C_{n,d} \right\rangle \right|^{2}$$

$$= \frac{1}{d^{n}} \left| \sum_{k_{1}, \dots, k_{n} = 0}^{d-1} \omega^{k_{1} k_{2} + \dots + k_{n-1} k_{n}} \frac{1}{\sqrt{d^{(n+1)/2}}} \sum_{l_{1}, l_{3}, \dots, l_{n} = 0}^{d-1} \omega^{-(l_{1} q_{1} + l_{3} q_{3} + \dots + l_{n} q_{n})} \left\langle l_{1} p_{2} l_{3} \dots l_{n} | k_{1} k_{2} k_{3} \dots k_{n} \right\rangle \right|^{2},$$

$$= \frac{1}{d^{\frac{n-1}{2}}} \delta_{p_{2} \oplus q_{1}, 0} \delta_{p_{2} \oplus p_{4} \oplus q_{3}, 0} \dots \delta_{p_{n-1} \oplus q_{n}, 0}.$$
(F7)

As for even n, this probability distribution is non-zero for all outcome tuples appearing in the first term in (F1): the only difference with the n-even case is in the number of non-zero terms in the distribution. Therefore, also for n-odd we recover the result in (F4).

For the second term in (F1), we calculate the probability distribution related to measurements of the $\frac{n+1}{2}$ subsystems $\{1,3,\ldots,n\}$ in the computational basis and measurements of the remaining $\frac{n-1}{2}$ subsystems $\{2,4,\ldots,n-1\}$ in the Fourier basis:

$$P(p_{1}, e_{q_{2}}, p_{3} \dots, e_{q_{n-1}}, p_{n} | C_{n,d}) = |\langle p_{1}e_{q_{2}}p_{3} \dots e_{q_{n-1}}p_{n} | C_{n,d} \rangle|^{2}$$

$$= \frac{1}{d^{n}} \left| \sum_{k_{1}, \dots, k_{n} = 0}^{d-1} \omega^{k_{1}k_{2} + \dots + k_{n-1}k_{n}} \frac{1}{\sqrt{d^{(n-1)/2}}} \sum_{l_{2}, l_{4}, \dots, l_{n-1} = 0}^{d-1} \omega^{-(l_{2}q_{2} + l_{4}q_{4} + \dots + l_{n-1}q_{n-1})} \langle p_{1}l_{2}p_{3} \dots p_{n} | k_{1}k_{2}k_{3} \dots k_{n} \rangle \right|^{2}, \quad (F8)$$

$$= \frac{1}{d^{\frac{n+1}{2}}} \delta_{p_{1} \oplus p_{3} \oplus q_{2}, 0} \delta_{p_{3} \oplus p_{5} \oplus q_{4}, 0} \dots \delta_{p_{n-2} \oplus p_{n} \oplus q_{n-1}, 0}.$$

This allows us to recover (F6) also for the n-odd case.

• Show that the spectral decomposition of $O_{n,d}^{cluster}$ is $\lambda(O_{n,d}^{cluster}) = \{\lambda_{C_{n,d}}, \lambda_2, \dots, \lambda_{d^n}\}$ such that $\lambda_i \leq 1 \quad \forall i \neq C_{n,d}$

We can use the same procedure presented in the second step of Appendix C for the GHZ witness operator. Therefore, after realizing that

$$O_{n,d}^{\text{cluster}} = 2 \left| C_{n,d} \right\rangle \left\langle C_{n,d} \right| + \sum_{i=2}^{d^n} \lambda_i \left| \lambda_i \right\rangle \left\langle \lambda_i \right|, \tag{F9}$$

we can prove that the shifted operator $\tilde{O}_{n,d}^{\text{cluster}} = O_{n,d}^{\text{cluster}} - C_{n,d}$ is a projector. Also in this case we can calculate its square,

$$(\tilde{O}_{n,d}^{\text{cluster}})^2 = (O_{n,d}^{\text{cluster}})^2 + C_{n,d} - \{O_{n,d}^{\text{cluster}}, C_{n,d}\} = (O_{n,d}^{\text{cluster}})^2 - 3C_{n,d}, \tag{F10}$$

and focus on the $(O_{n,d}^{\mathrm{cluster}})^2$ term. From the definition (F1) we get

$$(O_{n,d}^{\text{cluster}})^{2} = \left[\bigotimes_{l \text{ odd}} \sum_{q_{l}, p_{l+1} = 0}^{d-1} |e_{q_{l}} p_{l+1}| \langle e_{q_{l}} p_{l+1} | \delta_{p_{l+1} \oplus p_{l-1} \oplus q_{l}, 0} + \bigotimes_{l \text{ odd}} \sum_{p_{l}, q_{l+1} = 0}^{d-1} |p_{l} e_{q_{l+1}}| \langle p_{l} e_{q_{l+1}} | \delta_{p_{l} \oplus p_{l+2} \oplus q_{l+1}, 0} \right] \cdot \left[\bigotimes_{l \text{ odd}} \sum_{q'_{l}, p'_{l+1} = 0}^{d-1} |e_{q'_{l}} p'_{l+1}| \langle e_{q'_{l}} p'_{l+1} | \delta_{p'_{l+1} \oplus p'_{l-1} \oplus q'_{l}, 0} + \bigotimes_{l \text{ odd}} \sum_{p'_{l}, q'_{l+1} = 0}^{d-1} |p'_{l} e_{q'_{l+1}}| \langle p'_{l} e_{q'_{l+1}} | \delta_{p'_{l} \oplus p'_{l+2} \oplus q'_{l+1}, 0} \right],$$
(F11)

where the non-mixing terms produce again $O_{n,d}^{\text{cluster}}$ because of the orthonormality of both computational and Fourier basis. We can separately look at the mixing terms. From the first one we get

$$\bigotimes_{\substack{l \text{ odd} \\ p'_{l}, p'_{l+1} = 0 \\ p'_{l}, q'_{l+1} = 0}}^{d-1} \left\langle p'_{l} e_{q'_{l+1}} \middle| e_{q_{l}} p_{l+1} \right\rangle \middle| e_{q_{l}} p_{l+1} \middle| \left\langle p'_{l} e_{q'_{l+1}} \middle| \delta_{p_{l+1} \oplus p_{l-1} \ominus q_{l}, 0} \delta_{p'_{l} \oplus p'_{l+2} \ominus q'_{l+1}, 0}, \right.$$

$$= \frac{1}{\sqrt{d^{n}}} \bigotimes_{\substack{l \text{ odd} \\ p'_{l}, q'_{l+1} = 0}}^{n} \sum_{\substack{l \text{ odd} \\ p'_{l}, q'_{l+1} = 0}}^{d-1} \omega^{q_{l} p'_{l} - p_{l+1} q'_{l+1}} \middle| e_{q_{l}} p_{l+1} \middle| \left\langle p'_{l} e_{q'_{l+1}} \middle| \delta_{p_{l+1} \oplus p_{l-1} \ominus q_{l}, 0} \delta_{p'_{l} \oplus p'_{l+2} \ominus q'_{l+1}, 0}. \right.$$
(F12)

We can use the conditions imposed by the delta functions and rewrite the exponential term as

$$\omega^{q_l p'_l - p_{l+1} q'_{l+1}} = \omega^{(p_{l+1} + p_{l-1}) p'_l - p_{l+1} q'_{l+1} \pm p_{l+1} p'_{l+2}} = \omega^{p_{l+1} (p'_l + p'_{l+2} - q'_{l+1})} \omega^{p_{l-1} p'_l - p_{l+1} p'_{l+2}}, \tag{F13}$$

where the first exponential simplifies when we insert it into (F12) because of the condition imposed by the second delta, ending up with

$$\frac{1}{\sqrt{d^n}} \bigotimes_{\substack{l \text{ odd} \\ p'_{l}, q'_{l+1} = 0}}^{d-1} \sum_{\substack{l=0 \\ p'_{l}, q'_{l+1} = 0}}^{d-1} \omega^{p_{l-1}p'_{l} - p_{l+1}p'_{l+2}} \left| e_{q_{l}} p_{l+1} \right\rangle \left\langle p'_{l} e_{q'_{l+1}} \left| \delta_{p_{l+1} \oplus p_{l-1} \ominus q_{l}, 0} \delta_{p'_{l} \oplus p'_{l+2} \ominus q'_{l+1}, 0} \right. \right.$$
(F14)

In addition, we can realize that, once we take the tensor product over the odd l, all the exponents simplify:

$$n\text{-odd}: \quad p_{l-1}p'_{l} - p_{l+1}p'_{l+2} = \underbrace{0 - p_{2}p'_{3}}_{l=1} + \underbrace{p_{2}p'_{3} + p_{4}p'_{5}}_{l=3} + \cdots + \underbrace{p_{n-3}p'_{n-2} - p_{n-1}p'_{n}}_{l=n-2} + \underbrace{p_{n-1}p'_{n} - 0}_{l=n} = 0,$$

$$n\text{-even}: \quad p_{l-1}p'_{l} - p_{l+1}p'_{l+2} = \underbrace{0 - p_{2}p'_{3}}_{l=1} + \underbrace{p_{2}p'_{3} + p_{4}p'_{5}}_{l=3} + \cdots + \underbrace{p_{n-4}p'_{n-3} - p_{n-2}p'_{n-1}}_{l=n-3} + \underbrace{p_{n-2}p'_{n-1} - 0}_{l=n-1} = 0.$$
(F15)

Therefore, the whole exponential term in (F14) simplifies and we end up with

$$\frac{1}{\sqrt{d^{n}}} \bigotimes_{l \text{ odd}}^{n} \left(\sum_{q_{l}, p_{l+1} = 0}^{d-1} \delta_{p_{l+1} \oplus p_{l-1} \ominus q_{l}, 0} |e_{q_{l}} p_{l+1} \rangle \right) \left(\sum_{p'_{l}, q'_{l+1} = 0}^{d-1} \delta_{p'_{l} \oplus p'_{l+2} \ominus q'_{l+1}, 0} \left\langle p'_{l} e_{q'_{l+1}} \right| \right). \tag{F16}$$

By looking at the statistics derived in (F3) and (F5) for n even and in (F7) and (F8) for n odd, we can realize that the last result is precisely the $|C_{n,d}\rangle\langle C_{n,d}|$ projector.

The same procedure can be used for the second mixing term:

$$\bigotimes_{\substack{l \text{ odd } p_{l}, q_{l+1} = 0 \\ q'_{l}, p'_{l+1} = 0}}^{d-1} \left\langle p_{l} e_{q_{l+1}} \middle| e_{q'_{l}} p'_{l+1} \right\rangle \middle| p_{l} e_{q_{l+1}} \middle| \left\langle e_{q'_{l}} p'_{l+1} \middle| \delta_{p_{l} \oplus p_{l+2} \ominus q_{l+1}, 0} \delta_{p'_{l+1} \oplus p'_{l-1} \ominus q'_{l}, 0}, \right.$$
(F17)

since we can realize that it is precisely the first mixing term with $(p,q) \to (p',q')$.

Therefore, by inserting these results into (F10), we get

$$(\tilde{O}_{n,d}^{\text{cluster}})^2 = (O_{n,d}^{\text{cluster}})^2 - 3C_{n,d} = O_{n,d}^{\text{cluster}} - C_{n,d} = \tilde{O}_{n,d}^{\text{cluster}}, \tag{F18}$$

which proves that $\tilde{O}_{n,d}^{\mathrm{cluster}}$ is a projector.

• Derivation of the upper bound for $\mathcal{W}_{n,d}^{\text{cluster}}(\rho) = \operatorname{tr}\left(\rho O_{n,d}^{\text{cluster}}\right)$

The procedure for this step is identical to the one presented in Appendix C, since also in this case it is possible to use that

$$\lambda(O_{n,d}^{cluster}) = \{2, \lambda_2, \dots, \lambda_{d^n} : \lambda_i \le 1\} \quad \Longrightarrow \quad C_{n,d} + \sum_{i=2}^{d^n} \lambda_i |\lambda_i\rangle\langle\lambda_i| \le \mathbb{1}$$
 (F19)

to bound the witness as

$$W_{n,d}^{\text{cluster}}(\rho) = \operatorname{tr}\left(\rho O_{n,d}^{\text{cluster}}\right) = F_{\text{cluster}}(\rho) + \operatorname{tr}\left(\rho\left(C_{n,d} + \sum_{i=2}^{d^n} \lambda_i \left|\lambda_i\right\rangle \left|\lambda_i\right|\right)\right) \le F_{\text{cluster}}(\rho) + 1.$$
 (F20)

We can realize that $F_{\text{cluster}}(\rho)$ is the fidelity between a n-partite pure linear cluster state and a state ρ with $\mathcal{D}_{\text{GME}}(\rho) \leq d_{\text{GME}}$ that can be bounded by using Result 1 as shown in (B11). By inserting this result into (F20) we get:

$$W_{n,d}^{\text{cluster}}(\rho) \le 1 + \frac{d_{\text{GME}}}{d}.$$
 (F21)

Moreover, by looking at the last inequality in (F20) we can realize that:

$$F_{\text{cluster}}(\rho) \ge \mathcal{W}_{n,d}^{\text{cluster}}(\rho) - 1.$$
 (F22)

Appendix G: Reduction of the SDP to LP

Define the r-positive generalised reduction map $\Lambda(X)=\operatorname{tr} X 1\!\!1 - \frac{1}{r}X$ and the unnormalised states $\tilde{\sigma}_{S|\bar{S}}=q_{S|\bar{S}}\sigma_{S|\bar{S}}$. Then it is possible to show that, if ρ is a pure state, the following semidefinite program,

$$\max_{v,\tilde{\sigma}} v$$
s.t.
$$v\rho + \frac{1-v}{d^n} \mathbb{1} = \sum_{S|\bar{S}} \tilde{\sigma}_{S|\bar{S}},$$

$$\tilde{\sigma}_{S|\bar{S}} \ge 0 \quad \forall (S|\bar{S}),$$

$$(\Lambda_S \otimes \mathbb{1}_{\bar{S}})[\tilde{\sigma}_{S|\bar{S}}] \ge 0 \quad \forall (S|\bar{S}),$$

can be reduced to a linear program by representing it in a basis $\{|a_1 \dots a_n\rangle^D\}$, with $\{a_1, \dots, a_n\} \in \{0, \dots, d-1\}$, that we define as state-diagonal since the first element $|0 \dots 0\rangle^{D} \langle 0 \dots 0|$ is equal to the state ρ . Let U be the unitary that maps ρ expressed in the computational basis into the same state ρ expressed in this new basis, i.e. $U\rho U^{\dagger} = |0 \dots 0\rangle^{D} \langle 0 \dots 0|$. Then (G1) is equivalent to the following program,

$$\max_{v,\tilde{\sigma}} v$$
s.t. $vU\rho U^{\dagger} + \frac{1-v}{d^n} \mathbb{1} = \sum_{S|\bar{S}} U\tilde{\sigma}_{S|\bar{S}} U^{\dagger},$

$$U\tilde{\sigma}_{S|\bar{S}} U^{\dagger} \ge 0 \quad \forall (S|\bar{S}),$$

$$(\Lambda_S \otimes \mathbb{1}_{\bar{S}})[U\tilde{\sigma}_{S|\bar{S}} U^{\dagger}] \ge 0 \quad \forall (S|\bar{S}).$$
(G2)

Here, $U\rho U^{\dagger}$ is diagonal and w.l.g. therefore optimally chooses $U\tilde{\sigma}_{S|\bar{S}}U^{\dagger}$ diagonal as well. Since all the matrices are diagonal, this is in fact a linear program.

To prove this result it is enough to show that all the constraints in (G1) imply the constraints in (G2). Since for the first constraint this can be shown by simply using the unitarity of U, we will directly focus on the other two:

$$\bullet \ \tilde{\sigma}_{S|\bar{S}} \geq 0 \quad \implies \quad U \tilde{\sigma}_{S|\bar{S}} U^\dagger \geq 0$$

We can remember that the terms $U\tilde{\sigma}_{S|\bar{S}}U^{\dagger}$ are diagonal in the new basis, therefore:

$$U\tilde{\sigma}_{S|\bar{S}}U^{\dagger} = \sum_{a_1,\dots,a_n=0}^{d-1} {}^{D}\langle a_1\dots a_n | \tilde{\sigma}_{S|\bar{S}} | a_1\dots a_n \rangle^{D} \quad |a_1\dots a_n\rangle\langle a_1\dots a_n| \ge 0,$$
 (G3)

since, being $\tilde{\sigma}_{S|\bar{S}} \geq 0$ positive semidefinite, for any basis element we have ${}^D \langle a_1 \dots a_n | \tilde{\sigma}_{S|\bar{S}} | a_1 \dots a_n \rangle^D \geq 0$.

•
$$(\Lambda_S \otimes \mathbb{1}_{\bar{S}})[\tilde{\sigma}_{S|\bar{S}}] \geq 0 \implies (\Lambda_S \otimes \mathbb{1}_{\bar{S}})[U\tilde{\sigma}_{S|\bar{S}}U^{\dagger}] \geq 0$$

First, we can use the definition of our r-positive generalised reduction map and write

$$(\Lambda_S \otimes \mathbb{1}_{\bar{S}})[\tilde{\sigma}_{S|\bar{S}}] = \mathbb{1}_S \otimes \operatorname{tr}_S(\tilde{\sigma}_{S|\bar{S}}) - \frac{1}{r}\tilde{\sigma}_{S|\bar{S}} \ge 0.$$
 (G4)

Then, we for any bipartition $(S|\bar{S})$ the states in the new basis can be expressed as $|a_1 \dots a_n\rangle^D = |a_1 \dots a_S\rangle^D_S \otimes |a_{S+1} \dots a_n\rangle^D_{\bar{S}}$ and therefore we can explicitly calculate

$$\mathbf{1}_{S} \otimes \operatorname{tr}_{S}(U\tilde{\sigma}_{S|\bar{S}}U^{\dagger}) = \mathbf{1}_{S} \otimes \sum_{a_{1},\dots,a_{n}=0}^{d-1} {}^{D} \langle a_{1} \dots a_{n} | \tilde{\sigma}_{S|\bar{S}} | a_{1} \dots a_{n} \rangle^{D} \operatorname{tr}_{S}(|a_{1} \dots a_{n}\rangle^{D} \langle a_{1} \dots a_{n}|)$$

$$= \sum_{b_{1},\dots,b_{S}=0}^{d-1} |b_{1} \dots b_{S}\rangle_{S}^{D} {}^{D} \langle b_{1} \dots b_{S}| \otimes \sum_{a_{1},\dots,a_{n}=0}^{d-1} {}^{D} \langle a_{1} \dots a_{n} | \tilde{\sigma}_{S|\bar{S}} |a_{1} \dots a_{n}\rangle^{D} |a_{S+1} \dots a_{n}\rangle_{S}^{D} {}^{D} \langle a_{S+1} \dots a_{n}|, \tag{G5}$$

in which we can rename $|a_1\dots a_S\rangle_S^D \leftrightarrow |b_1\dots b_S\rangle_S^D$ to get

$$= \sum_{a_1,\dots,a_n=0}^{d-1} \sum_{b_1,\dots,b_S=0}^{d-1} \sum_{S}^{D} \langle b_1 \dots b_S | \frac{D}{S} \langle a_{S+1} \dots a_n | \tilde{\sigma}_{S|\bar{S}} | b_1 \dots b_S \rangle_{S}^{D} | a_{S+1} \dots a_n \rangle_{\bar{S}}^{D} \quad |a_1 \dots a_n \rangle^{D} \langle a_1 \dots a_n |$$

$$= \sum_{a_1,\dots,a_n=0}^{d-1} {}^{D} \langle a_1 \dots a_n | \mathbb{1}_{S} \otimes \operatorname{tr}_{S}(\tilde{\sigma}_{S|\bar{S}}) | a_1 \dots a_n \rangle^{D} | a_1 \dots a_n \rangle^{D} \langle a_1 \dots a_n |,$$
(G6)

where in the last equality we used the definition of the partial trace. In conclusion,

$$(\Lambda_{S} \otimes \mathbb{1}_{\bar{S}})[U\tilde{\sigma}_{S|\bar{S}}U^{\dagger}] = \mathbb{1}_{S} \otimes \operatorname{tr}_{S}(U\tilde{\sigma}_{S|\bar{S}}U^{\dagger}) - \frac{1}{r}U\tilde{\sigma}_{S|\bar{S}}U^{\dagger}$$

$$= \sum_{a_{1} \dots a_{n}=0}^{d-1} {}^{D}\langle a_{1} \dots a_{n} | \left(\mathbb{1}_{S} \otimes \operatorname{tr}_{S}(\tilde{\sigma}_{S|\bar{S}}) - \frac{1}{r}\tilde{\sigma}_{S|\bar{S}} \right) |a_{1} \dots a_{n}\rangle^{D} |a_{1} \dots a_{n}\rangle^{D} \langle a_{1} \dots a_{n} |,$$
(G7)

which implies that $(\Lambda_S \otimes 1\!\!1_{\bar{S}})[U\tilde{\sigma}_{S|\bar{S}}U^\dagger] \geq 0$ if $(\Lambda_S \otimes 1\!\!1_{\bar{S}})[\tilde{\sigma}_{S|\bar{S}}] \geq 0$.

Appendix H: Tables of critical visibilities from linear programming

In the table below, we present the bounds on the critical visibility obtained from solving the linear program presented in the main text and Appendix G. All computations were made on a standard desktop computer⁶. Our case studies are based on the n-partite d-dimensional GHZ states $|\text{ghz}_{n,d}\rangle$ and linear cluster states $|C_{n,d}\rangle$.

For GHZ states and cluster states respectively, we define a state-diagonal basis, indicated as $\{|a_1...a_n\rangle^D\}$ with $\{a_1,...,a_n\} \in \{0,...,d-1\}$, in which $|\operatorname{ghz}_{n,d}\rangle$ and $|C_{n,d}\rangle$ are associated respectively to the first element, $|0...0\rangle^D$. By indicating with $\{|\psi_{a_1...a_n}\rangle\}$ the vectors of the state-diagonal basis expressed in the computational basis, we can define the unitary, U, that maps a state from the computational basis to its state-diagonal basis:

$$\begin{cases} \text{GHZ-case:} & |\psi_{a_1...a_n}\rangle = Z^{a_1} \otimes X^{a_2} \otimes \cdots \otimes X^{a_n} \left| \text{ghz}_{n,d} \right\rangle \\ \text{Cluster-case:} & |\psi_{a_1...a_n}\rangle = Z^{a_1} \otimes \cdots \otimes Z^{a_{n-2}} \otimes X^{a_{n-1}} \otimes X^{a_n} \left| C_{n,d} \right\rangle \end{cases} \implies U = \sum_{a_1,...,a_n=0}^{d-1} |a_1 \dots a_n\rangle \langle \psi_{a_1...a_n}|.$$
(H1)

Moreover, to get more accurate results, we applied the generalised reduction map on both sets of each bipartition, i.e. we evaluated

$$\max_{v,\tilde{\sigma}} v$$
s.t.
$$v U \rho U^{\dagger} + \frac{1 - v}{d^{n}} \mathbf{1} = \sum_{S|\bar{S}} U \tilde{\sigma}_{S|\bar{S}} U^{\dagger},$$

$$U \tilde{\sigma}_{S|\bar{S}} U^{\dagger} \ge 0 \quad \forall (S|\bar{S}),$$

$$(\Lambda_{S} \otimes \mathbf{1}_{\bar{S}}) [U \tilde{\sigma}_{S|\bar{S}} U^{\dagger}] \ge 0 \quad \forall (S|\bar{S}),$$

$$(\mathbf{1}_{S} \otimes \Lambda_{\bar{S}}) [U \tilde{\sigma}_{S|\bar{S}} U^{\dagger}] \ge 0 \quad \forall (S|\bar{S}).$$
(H2)

From the table of results, it is seen that in all considered cases, the cluster state is more noise tolerant than the GHZ state.

⁶ The results have been computed on the following desktop:

[•] CPU: AMD Ryzen 9 5900X 12-Core Processor 3.70 GHz;

TABLE III: LP results - GHZ state and cluster state

(1)	D ()	(I D)	(I D)	(C 1 1'4)			
(n,d)	$\mathcal{D}_{ ext{GME}}(ho)$	v _{ghz} (LP)	$v_{\rm cluster}$ (LP)	v (fidelity)			
(3,2)	1	0.4286	*	0.4286			
(3,3)	1	0.2500	*	0.3077			
(3,3)	2	0.5909	*	0.6538			
(3,4)	1	0.1579	*	0.2381			
(3,4)	2	0.3725	*	0.4921			
(3,4)	3	0.6444	*	0.7460			
(3,5)	1	0.1071	*	0.1935			
(3,5)	2	0.2500	*	0.3951			
(3,5)	3	0.4318	*	0.5967			
(3,5)	4	0.6711	*	0.7984			
(4,2)	1	0.4667	0.4146	0.4667			
(4,3)	1	0.2703	0.2174	0.3250			
(4,3)	2	0.6029	0.5129	0.6625			
(4,4)	1	0.1688	0.128	0.2471			
(4,4)	2	0.3816	0.294	0.4980			
(4,4)	3	0.6503	0.534	0.7490			
(4,5)	1	0.1135	_	0.1987			
(4,5)	2	0.2560	_	0.3990			
(4,5)	3	0.4369	_	0.5994			
(4,5)	4	0.6745	_	0.7997			
(5,2)	1	0.4839	_	0.4839			
(5,3)	1	0.2358	-	0.3306			
(5,3)	2	0.5549	_	0.6653			
(5,4)	1	0.1203	_	0.2493			
(5,4)	2	0.2918	_	0.4995			
(5,4)	3	0.5532		0.7498			

Critical visibility, v, from convex programming relaxation for the GME-dimension. Case study presented for target GHZ states and cluster states under white noise. These states are local-unitary equivalent for n=3, while in all the other cases, the cluster state is more noise tolerant than GHZ. The "-" indicates the cases in which our desktop was not able to evaluate the linear program.